Food & Function

ROYAL SOCIETY OF CHEMISTRY

PAPER

View Article Online
View Journal

Check for updates

Cite this: DOI: 10.1039/d1fo01421h

Inhibitory effect of paeoniflorin on IgE-dependent and IgE-independent mast cell degranulation *in vitro* and *vivo*

Yang Zhao,[a] Xiangsheng Li,[a] Jianzhou Chu,[b] Yuxin Shao,[a] Yizhao Sun,[a] Yanfen Zhang *[c] and Zhongcheng Liu *[a]

The incidence of allergic diseases has increased to such a point that they have become common and have reached epidemic levels. However, their pathogenesis is not fully understood. Paeoniae Radix Rubra is a traditional Chinese medicine that is also used as a dietary supplement. Its main active ingredient is paeoniflorin. Paeoniflorin has good anti-inflammatory, immunomodulation, and antitumor effects. It is utilized in the treatment of various diseases in clinical settings. However, its effects on type I allergies and pseudoallergic reactions have not been comprehensively studied. In this study, we aimed to use DNP-IgE/DNP-BSA and C48/80 to simulate type I allergies and pseudoallergic reactions to evaluate the therapeutic effects of paeoniflorin to these diseases and identify its molecular mechanisms in cell degranulation both *in vivo* and *in vitro*. Results showed that paeoniflorin inhibited the degranulation of RBL-2H3 cells induced by these two stimuli (IgE-dependent and IgE-independent stimuli) in a dose-dependent manner. Moreover, qPCR and western blot analyses indicated that paeoniflorin may regulate the IgE/FcεR I, MRGPRB3, and downstream signal transduction pathways to exert its therapeutic effects on type I allergies and pseudoallergic reactions. In addition, DNP-IgE/DNP-BSA and compound 48/80 were used to induce the establishment of a passive cutaneous anaphylaxis mouse model. Paeoniflorin was found to suppress the extravasation of Evans Blue and tissue edema in the ears, back skin, and paws of the mice. This result further confirmed that paeoniflorin has a notable therapeutic effect on type I allergies and pseudoallergic reactions. Therefore, paeoniflorin could potentially be used as a drug for the treatment of type I allergies and pseudoallergic reactions. This study provides new insights into expanding the treatment range of paeoniflorin and its pharmacological mechanism.

Received 7th May 2021,
Accepted 25th June 2021

DOI: 10.1039/d1fo01421h

rsc.li/food-function

Published on 26 June 2021. Downloaded on 7/6/2021 4:12:49 AM.

1. Introduction

In recent years, the incidence of allergic diseases has increased to such a point that they have become common and have reached epidemic levels. Approximately 20%–30% of the world's population suffers from allergic diseases. The mechanisms of allergy formation and maintenance are extremely complicated. The specific pathogenesis of these diseases remains unclear, and no method that can completely cure them has been developed thus far. These limitations pose severe challenges to research on these diseases and their clinical treatment. On the basis of their pathogenesis, allergies are classified into four types, of which type I allergies are the most common in clinical settings. Type I allergies are also called allergic reactions, which are an immediate type and mediated by immunoglobulin E (IgE-dependent).[1]

As the main response cells in allergic diseases, mast cells (MCs) can degranulate to release allergic mediators, such as histamine (HA), β-hexosaminidase (β-Hex), 5-hydroxytryptamine (5-HT), and prostaglandins, all of which can cause allergic diseases. The stimuli that induce MC degranulation can be divided into two categories: immune stimuli and nonimmune stimuli. Immune stimuli are mainly caused by specific antigens, such as the binding of IgE and FcεR I to induce MC degranulation. By comparison, nonimmune stimuli, such as compound 48/80 (C48/80), can directly activate MC degranulation, resulting in clinical symptoms similar to those of type I allergies, which are called pseudoallergic reactions. Pseudoallergic reactions are mediated through an IgE-indepen-

[a]College of Pharmaceutical Sciences, Key Laboratory of Pharmaceutical Quality Control of Hebei Province, Institute of Life Science and Green Development, Hebei University, Baoding, 071002, China. E-mail: liuzc@hbu.edu.cn; Tel: +86-312-5971107
[b]College of Life Sciences, Hebei University, Baoding, 071002, China
[c]Technology Transfer Center, Hebei University, Baoding, 071002, China. E-mail: zhangjing@hbu.edu.cn; Tel: +86-312-5079483

View Article Online
该文档是极速PDF编辑器生成，
http://www.jisupdfeditor.com/

Published on 26 June 2021. Downloaded on 7/6/2021 4:12:49 AM.

dent method. Pseudoallergic reactions belong to the scope of adverse drug reactions, a topic that has recently received increased attention.

In terms of mechanism, the occurrence of type I allergies is mediated by immune mechanism. Type I allergies do not appear to be related to dosage, and they do not respond to the first administration of anti-allergy drugs. Pseudoallergic reactions are a non-antigen antibody binding reaction caused by the direct stimulation or activation of the release of inflammatory mediators by anti-allergy drugs. This type of reaction has a certain relationship to dosage and can occur at the first administration of the drug. The mechanism of pseudoallergic reactions remains unclear.[2,3] In clinical treatment, pseudoallergic reactions are often confused with allergic reactions. Although the mechanisms of the two are different, pseudoallergic reactions and type I allergies are both related to the degranulation of MC and basophils to release HA and other biologically active mediators. Both of them belong to immediate allergic reactions, and they require considerably different clinical prevention and treatment strategies. Therefore, clarifying the nature and characteristics of allergic reactions is very important to ensure the safety of clinical drugs. Glucocorticoids and antihistamines are often used to treat allergic diseases, but they have short curative effects and results in many adverse reactions. Therefore, the characteristics of traditional Chinese medicines with multiple targets, multiple curative effects, and few adverse reactions have attracted increased attention. Traditional Chinese medicines have a long history of being used to treat allergic diseases. However, owing to the complex chemical components and pharmacological effects of traditional Chinese medicines, their specific active ingredients and mechanisms remain unknown. This gap in research poses a huge challenge in studying the mechanisms of traditional Chinese medicines for the treatment of allergic reactions. In recent years, as traditional Chinese medicines are comprehensively explored and with the development of related technologies, the use of traditional Chinese medicines for the treatment of allergic diseases has gained traction. Various traditional Chinese medicines and their extracts, such as polydatin, glycyrrhizic acid, and quercitrin, have been found to have therapeutic effects on allergic reactions.[4–6] Traditional Chinese medicines offer a huge potential to the research and development of new drugs. Moreover, they have good application prospects in the treatment of allergic diseases. Nevertheless, numerous traditional Chinese medicines and ingredients with anti-allergic activity have yet to be explored, among which is paeoniflorin (Pae), which has anti-inflammatory and immunomodulatory effects.

Paeoniae Rubra Radix is the dried roots of *Paeonia lactiflora* Pall or *Paeonia veitchii* Lynch of Family Ranunculaceae. Paeoniae Rubra Radix is listed by the National Health Commission of the People's Republic of China as one of the traditional Chinese medicines that can be used as a dietary supplement. It has a long history of application and a wide range of uses. Paeoniae Rubra Radix contains terpenoids and their glycosides, flavonoids and their glycosides, and other chemical components, and its main active ingredient is Pae.[7] Research on the chemical components and immunomodulatory and anti-inflammatory mechanisms of Paeoniae Rubra Radix mainly focuses on Pae, which has various effects, such as anti-inflammatory and immunomodulatory effects, sedation, analgesia, and improvement of cognitive ability.[8–11] In addition, Pae is one of the monomer components in the classic prescription of Siwu Decoction, Shaoyao Gancao Decoction, and Xiaoqinglong Decoction for the treatment of allergic diseases. Thus, Pae may have anti-allergic effects. Several studies reported that Pae can inhibit type I allergies and pseudoallergic reactions. However, the use of Pae for the treatment of these diseases has not been compared and systematically analyzed; moreover, its in-depth pharmacological mechanism must be further explored.[12,13]

In this study, we used DNP-IgE/DNP-BSA and C48/80 to induce MCs degranulation in a passive cutaneous anaphylaxis (PCA) mouse model and in RBL-2H3 cells both *in vivo* and *in vitro* to simulate the processes of type I allergies and pseudoallergic reactions, respectively. The therapeutic effects of Pae on these diseases and its molecular mechanism were investigated. Results showed that Pae exerts an inhibitory effect on the degranulation of IgE-dependent and IgE-independent cells, indicating that this compound has notable therapeutic effects on type I allergies and pseudoallergic reactions. Therefore, Pae can be potentially developed as an anti-allergy drug.

2. Materials and methods

2.1. Materials and reagents

DNP-IgE, C48/80, 4-nitrophenyl-*N*-acetyl-β-D-galactosaminide and ketotifen fumarate were purchased from Sigma (St Louis, MO, USA). DNP-BSA purchased from Biosearch (Petaluma, CA, USA). RNAiso Plus, PrimeScript™ RT reagent Kit with gDNA Eraser, TB Green® Premix Ex Taq™ II were purchased from Takara (Beijing, China). AO/EB kit, CCK-8 kit, toluidine blue staining kit, BCA protein assay kit, primers and Evans Blue were purchased from Shenggong Biological Engineering Company (Shanghai, China). Rat histamine ELISA kit was purchased from Enzyme-linked Biotechnology Company (Shanghai, China). Fluo-4, F-127, DMEM medium and paeoniflorin (Purity ≥ 98%) were purchased from Solarbio Science & Technology Company (Beijing, China). Primary and secondary antibodies were purchased from Biosynthesis Biotechnology Company (Beijing, China). Fetal bovine serum was purchased from Invitrogen (Carlsbad, CA, USA). PVDF membrane and ECL kit were purchased from were purchased from Thermo Fisher Scientific Inc. (Waltham, MA, USA).

Rat basophilic leukemia cell line 2H3 (RBL-2H3) were obtained from the Cell Resource Center, Shanghai Institutes for Biological Sciences, Chinese Academy of Sciences (Shanghai, China). Female Kunming mice (SPF-grade, 6–8 weeks old, 35–40 g) were purchased from Beijing Vital River Laboratory Animal Technology Company (Beijing, China). All

This journal is © The Royal Society of Chemistry 2021

Published on 26 June 2021. Downloaded on 7/6/2021 4:12:49 AM.

mice were housed in the University Laboratory Animal Center, and this study was performed in strict accordance with the NIH Guidelines for the Care and Use of Laboratory Animals (NIH Publication no. 85-23 Rev.1985). The experimental protocols for using mice were approved by the Animal Ethics and Welfare Committee at Hebei University, Baoding, China (Permit Number: SYXK 2017-002).

2.2 Cell culture

DMEM medium (containing 10% fetal bovine serum, 100 U mL^{-1} penicillin and 100 μg mL^{-1} streptomycin) was used to culture RBL-2H3 cells. The cells were cultured in a 37 °C, 5% CO_2 incubator.

2.3 Cell viability assay

RBL-2H3 cells (1×10^5 cells per mL) were grown in 96-well plates with 100 μL per well. Normal group: cultured-with cells, and treated without Pae. Pae group: cultured with cells, and treated with Pae. Blank group: cultured without cells, and treated without Pae, and each group was designed in quintuplicate. After 24 h, the old medium was discarded, and the complete medium containing different concentrations of Pae (0.5, 2.5, 5, 25, 50, 125, 250 μg mL^{-1}) was added to the Pae group. After 23 h, each group added 10 μL of CCK-8 reagent and reacted for 1 h, and the absorbance was measured at 405 nm by using the microplate reader (Bio-Rad, Hercules, USA).

$$\text{Cell survival rate}(\%) = (\text{Pae group OD value} - \text{Blank group OD value})/(\text{Normal group OD value} - \text{Blank group OD value}) \times 100\%$$

2.4 Toluidine blue staining assay

RBL-2H3 cells (6×10^5 cells per mL) were grown in 24-well plates with 1 mL per well. Normal group: cell sensitization, no stimulation, no treatment with Pae or ketotifen fumarate (Keto). Model group: cell sensitization, stimulation, no treatment with Pae or Keto. Pae group: cell sensitization, stimulation, Pae concentration was 0.5, 2.5, 5 μg mL^{-1}. Keto group: cell sensitization, stimulation, Keto concentration was 25 μg mL^{-1}, and each group was designed in triplicate. After 24 h, the cells were washed with PBS. Each well was sensitized by adding 500 μL of DNP-IgE (0.2 μg mL^{-1}). After 12 h, Pae and Keto group were replaced with 1 mL of the corresponding concentration of the drug respectively, and the rest of the group was replaced with the same amount of complete medium. After 1 h, the cells were washed with PBS. Except for Normal group, 200 μL of DNP-BSA (0.4 μg mL^{-1}) was added for stimulation, and Normal group was added with the same amount of PIPES buffer (subsequent experiment operation was the same). After 1 h, the reaction was terminated by ice bath for 10 min. Cell morphology was measured by using the toluidine blue staining kit according to the instructions.

2.5 β-Hex release assay

2.5.1 Induced by DNP-IgE/DNP-BSA. RBL-2H3 cells (3.5×10^5 cells per mL) were grown in 24-well plates with 1 mL per well. Negative control group: no sensitization, no stimulation, and the concentration was the same as that of the Pae or Keto group. The rest of the groups were the same as 2.4, and each group was designed in triplicate. After 24 h, the cells were washed with PBS. Except for Negative control group, each group was sensitized with 500 μL of DNP-IgE (0.2 μg mL^{-1}), and Negative control group was added with the same amount of complete medium. After 12 h, Negative control group, Pae group and Keto group were replaced with 1 mL of the drug respectively. After 1 h, the cells were washed with PBS. Model group, Pae group and Keto group were stimulated with 200 μL of DNP-BSA (0.4 μg mL^{-1}), and the other groups were given the same amount of PIPES buffer. After 1 h, the reaction was terminated by ice bath for 10 min. The supernatant was taken and centrifuged at 3000 rpm for 5 min. 50 μL of supernatant from each group was transferred to a 96-well plate, and 50 μL of chromogenic solution (1 mmol L^{-1} 4-nitrophenyl-*N*-acetyl-β-D-galactosaminide, pH = 4.5) was added. After 1 h, added 200 μL of stop solution (Na_2CO_3/$NaHCO_3$, pH = 10.7) to each well. The absorbance was measured at 405 nm.

$$\text{β-Hex release rate}(\%) = (\text{Drug group OD value} - \text{Negative control group OD value})/(\text{Model group OD value} - \text{Normal group OD value}) \times 100\%$$

2.5.2 Induced by C48/80. Cell culture was the same as 2.5.1. Normal group: added DMSO. Model group: added C48/80; Pae group: Pae concentration was 0.5, 2.5, 5 μg mL^{-1}, and added C48/80. Keto group: Keto concentration was 25 μg mL^{-1}, and added C48/80. Negative control group: the same concentration as the Pae group or Keto group, and added DMSO, and each group was designed in triplicate. After 24 h, the cells were washed with PBS. Negative control group, Pae group and Keto group were replaced with 1 mL of the drug respectively. After 1 h, the cells were washed with PBS. Model group, Pae group and Keto group were added with 200 μL of C48/80 (20 μg mL^{-1}), and the other groups were added with 200 μL of 2% DMSO. After 30 min, the reaction was terminated by ice bath for 10 min. The rest of the experiment steps were the same as section 2.5.1.

2.6 HA release assay

2.6.1 Induced by DNP-IgE/DNP-BSA. RBL-2H3 cells (3.5×10^5 cells per mL) were grown in 24-well plates with 1 mL per well. The method of cell culture and grouping was the same as 2.4. After 24 h, the cells were washed with PBS. Each group was sensitized with 500 μL of DNP-IgE (0.2 μg mL^{-1}). After 12 h, Pae and Keto group were replaced with 1 mL of the corresponding concentration of the drug respectively. Except for Normal group, 200 μL of DNP-BSA (0.4 μg mL^{-1}) was added for stimulation. After 30 min, the reaction was terminated by ice bath for 10 min. HA release rate was measured by using the rat histamine ELISA kit according to the instructions.

Published on 26 June 2021. Downloaded on 7/6/2021 4:12:49 AM.

2.6.2 Induced by C48/80. Cell culture was the same as 2.6.1. Normal group: added DMSO. Model group: added C48/80; Pae group: Pae concentration was 0.5, 2.5, 5 μg mL^{-1}, and added C48/80. Keto group: Keto concentration was 25 μg mL^{-1}, and added C48/80, and each group was designed in triplicate. After 24 h, the cells were washed with PBS. Pae group and Keto group were replaced with 1 mL of the drug respectively. After 1 h, except for Normal group, 200 μL of C48/80 (20 μg mL^{-1}) was added. After 30 min, the reaction was terminated by ice bath for 10 min. The rest of the experiment steps were the same as section 2.6.1.

2.7 Apoptosis assay

2.7.1 Induced by DNP-IgE/DNP-BSA. RBL-2H3 cells (1×10^6 cells per mL) were grown in 6-well plates with 2 mL per well. The method of cell culture and grouping was the same as 2.4. After 24 h, the cells were washed with PBS. Each group was sensitized with 1 mL of DNP-IgE (0.2 μg mL^{-1}). After 12 h, Pae and Keto group were replaced with 2 mL of the corresponding concentration of the drug respectively. Except for Normal group, 400 μL of DNP-BSA (0.4 μg mL^{-1}) was added for stimulation. After 1 h, the reaction was terminated by ice bath for 10 min. The cells were washed with PBS, stained the cells according to the instructions of the AO/EB kit, and observed with the fluorescence microscope (IX5, Olympus, Tokyo, Japan). Randomly observed and recorded 300 cells in 5 fields of view. Normal cells (VN): the nucleus is green with normal structure. Early apoptotic cells (VA): the nucleus is green with abnormal structure. Late apoptotic cells (NVA): the nucleus is orange-red with abnormal structure. Necrotic cell (NVN): The nucleus is orange-red with normal structure.

$$\text{Apoptosis rate}(\%) = (\text{VA} + \text{NVA})/(\text{VN} + \text{VA} + \text{NVA} + \text{NVN}) \times 100\%$$

2.7.2 Induced by C48/80. The cell culture was the same as section 2.7.1, and the grouping was the same as section 2.6.2. After 24 h, the cells were washed with PBS. Pae group and Keto group were replaced with 2 mL of the drug respectively. After 1 h, except for Normal group, 400 μL of C48/80 (20 μg mL^{-1}) was added. After 30 min, the reaction was terminated by ice bath for 10 min. The remaining steps were the same as section 2.7.1.

2.8 Ca^{2+} concentration assay

2.8.1 Induced by DNP-IgE/DNP-BSA. RBL-2H3 cells (2.5×10^5 cells per mL) were grown in 12-well plates with 2 mL per well. The method of cell culture and grouping was the same as 2.4. After 24 h, the cells were washed with PBS. Each group was sensitized with 500 μL of DNP-IgE (0.2 μg mL^{-1}). After 12 h, Pae and Keto group were replaced with 2 mL of the corresponding concentration of the drug respectively. After 1 h, the cells were washed with HBSS. Each group added 200 μL of HBSS (4 μM Fluo-4, AM). After 20 min, added 1 mL of HBSS (1% fetal bovine serum). After 40 min, except for Normal group, 200 μL of DNP-BSA (0.4 μg mL^{-1}) was added for stimulation. Then immediately observed the fluorescence at 494 nm and photographed by the fluorescence microscope.

2.8.2 Induced by C48/80. The cell culture was the same as section 2.8.1, and the grouping was the same as section 2.6.2. After 24 h, the cells were washed with PBS. Pae group and Keto group were replaced with 2 mL of the drug respectively. After 1 h, except for Normal group, 200 μL of C48/80 (20 μg mL^{-1}) was added. After 30 min, the cells were washed with HBSS. The remaining steps were the same as section 2.8.1.

2.9 Western blot analysis

RBL-2H3 cells (5×10^5 cells per mL) were grown in 6-well plates with 2 mL per well. The method of cell culture and grouping was the same as section 2.4. After 24 h, the cells were washed with PBS. Each group was sensitized with 1 mL of DNP-IgE (0.2 μg mL^{-1}). After 12 h, Pae and Keto group were replaced with 2 mL of the corresponding concentration of the drug respectively. Except for Normal group, 400 μL of DNP-BSA (0.4 μg mL^{-1}) was added for stimulation. After 30 min, the protein was extracted and the total protein concentration was measured by the BCA protein assay kit. Lyn, p-Lyn, Syk, p-Syk and β-actin were used as primary antibodies, and HRP-conjugated goat anti-rabbit IgG was used as secondary antibodies. ChemiDoc Imaging System (Bio-Rad, Hercules, USA) was used for imaging, and Image J software was used for densitometry analysis.

2.10 qPCR

The steps were the same as 2.9. After 1 h of stimulation, the reaction was terminated by ice bath for 10 min. RNAiso Plus kit extracted total RNA, and PrimeScript™ RT reagent Kit with gDNA Eraser removed genomic DNA from RNA and performed reverse transcription. Used TB Green® Premix Ex Taq™ II for qPCR reaction. (Pre-denaturation: 95 °C, 30 s. PCR reaction: 95 °C, 5 s; 60 °C, 30 s; 72 °C, 30 s; 40 cycles. Dissolution curve analysis: 95, 15 s; 55 °C, 15 s; 95 °C, 15 s). The primer design was as follows:

(1) Lyn-F: GCAGAGGGAATGGCATACATC, Lyn-R: GCAAGGCCAAAATCTGCAA;

(2) Syk-F: ACAATGGACTGAACCCTG, Syk-R: AGTAGCCTGAGCCAAGAA;

(3) Fyn-F: ACCACCAAAGGTGCCTACTC, Fyn-R: ATGTAGTACCCGCCGTTGT;

(4) PLCγ-F: GGACTATGGTGGGAAGAAGC, PLCγ-R: TTTGCCCTCAGGACGAAT;

(5) PI3K-F: ATACTTGATGTGGCTGACG; PI3K-R: CAATAGGTTCTCGGCTTT;

(6) Akt-F: TGGCACCGTCCTTGATACCC, Akt-R: CACGACCGCCTCTGCTTTGT;

(7) p38-F: GGACCTAAAGCCCAGCAA, p38-R: CAGCCCACGGACCAAATA;

(8) ERK-F: TCTCCCGCACAAAAATAAG, ERK-R: GGAAGGGGACAAACTGAAT;

(9) JNK-F: ACAATGGACTGAACCCTG, JNK-R: AGTAGCCTGAGCCAAGAA;

This journal is © The Royal Society of Chemistry 2021

Published on 26 June 2021. Downloaded on 7/6/2021 4:12:49 AM.

(10) p65-F: AACACTGCCGAGCTCAAGAT, p65-R: CATCGGCTTGAGAAAAGGAG;

(11) IL-4-F: ACGGAGATGGATGTGCCAAAC, IL-4-R: AGCACCTTGGAAGCCCTACAGA;

(12) IFN-γ-F: CGGCACAGTCATTGAAAGCCTA, IFN-γ-R: GGCACCACTAGTTGGTTGTCTTTG;

(13) ORAI-1-F: CCATTCTCTAACACCGGGCA, ORAI-1-R: GGTCATGGGGAAGGGCATAA;

(14) ORAI-2-F: CCATGAGTGCCGAGCTCAAT, ORAI-2-R: TGGTGGTTGGATGTGACCAG;

(15) GAPDH-F: CCCACTAACATCAAATGGGG, GAPDH-R: CCTTCCACAATGCCAAAGTT.

2.11 Passive cutaneous anaphylaxis

2.11.1 Induced by DNP-IgE/DNP-BSA. Female Kunming mice were randomly divided into 6 groups: Normal group, Model group, Pae group (25, 50, 100 mg kg^{-1}) and Keto group (20 mg kg^{-1}). DNP-IgE (0.5 μg) was intradermally injected into in the right ear, right paw and back skin of mice in Model group, Pae group and Keto group for sensitization, and the mice in Normal group were injected with the same volume of PBS. After 24 h, the Pae group and Keto group were given corresponding doses of drugs according to the body weight of mice. The other groups were given the corresponding volume of normal saline. After 1 h, except for Normal group, mice were intravenously injected with 200 μL of PBS (containing 0.5 mg of DNP-BSA and 1% Evans Blue). After 30 min, the mice were euthanized and photographed. Recorded the extravasation of Evans Blue from the ears, paws and back skin. The pigmented areas in ears of the same size around the injection site were taken, and the thickness was measured by vernier caliper and the degree of ear swelling was calculated. The balance weighed the weight of the paw after stimulation and the degree of paw swelling was calculated. Recorded the extravasation diameter of Evans Blue on the back skin.

The ears were soaked in 200 μL of formamide and placed in water bath at 85 °C for 2 h. Then, it was centrifuged at 3000 rpm for 10 min, and the supernatant was taken to detect the absorbance at 620 nm. Cut the pigmented areas in paws and back skin of the same size around the injection site, and dried them at 60 °C for 24 h. Soaked them in 1 mL of formamide and placed them in a water bath at 85 °C for 2 h, centrifuge at 3000 rpm for 10 min, and the supernatant was taken to detect the absorbance at 620 nm.

$$\text{Ear swelling}(\%) = (\text{right ear thickness} - \text{left ear thickness})/\text{left ear thickness} \times 100\%$$

$$\text{Paw swelling}(\%) = (\text{right paw weight} - \text{left paw weight})/\text{left paw weight} \times 100\%$$

2.11.2 Induced by C48/80. The grouping of mice was the same as section 2.11.1, and the Pae group and Keto group were given corresponding doses of drugs according to the body weight of mice. The other groups were given the corresponding volume of normal saline. After 1 h, C48/80 (50 μg) was intradermally injected into in the right ear, right paw and back skin of mice in Model group, Pae group and Keto group, and the mice in Normal group were injected with the same volume of PBS. After 20 min, except for Normal group, mice were intravenously injected with 200 μL of PBS (containing 1% Evans Blue). After 30 min, the mice were euthanized, and the remaining operations and detection indicators were the same as section 2.11.1 (the process of animal experiments was shown in Fig. 1).

2.12 Statistical analysis

Results were expressed as the mean ± standard deviation (SD). A one-way analysis of variance (ANOVA) in SPSS 17.0 software

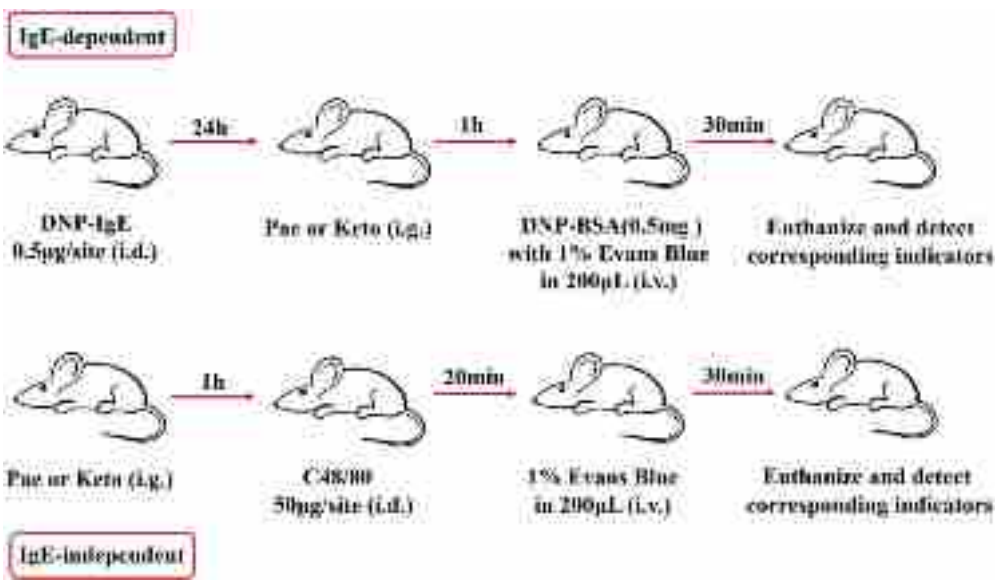

Fig. 1 Process of animal experiments.

Published on 26 June 2021. Downloaded on 7/6/2021 4:12:49 AM.

was used to assess significant differences between groups. $p < 0.05$ has a significant difference.

3. Results

3.1 Effects of Pae on the proliferation activity of RBL-2H3 cells

When the concentration of Pae was 0.5–5 μg mL^{-1}, it had no remarkable effect on cell proliferation. However, when the concentration of Pae was >25 μg mL^{-1}, it had a substantial inhibitory effect on cell proliferation. As its concentration further increased, its inhibitory effect also increased (Fig. 2). On the basis of the results, the concentrations of Pae selected for subsequent experiments were 0.5, 2.5, and 5 μg mL^{-1}.

3.2 Pae can inhibit morphological changes in RBL-2H3 cells during degranulation

Toluidine blue can bind to the nucleus of MCs and their particles to show different colors, a feature that can be used to judge the degree of MCs degranulation. MCs in the normal group were normal fusiform, blue-purple, and darkest in color. After degranulation, the cells in the Model group showed irregular shapes and became lighter in color. In the Pae group, the number of irregular cells were reduced, and the color of the cells became darker in a dose-dependent manner (Fig. 3), among which the morphology of MCs in the 2.5 and 5 μg mL^{-1} Pae groups was similar to that of the positive control group (Keto group).

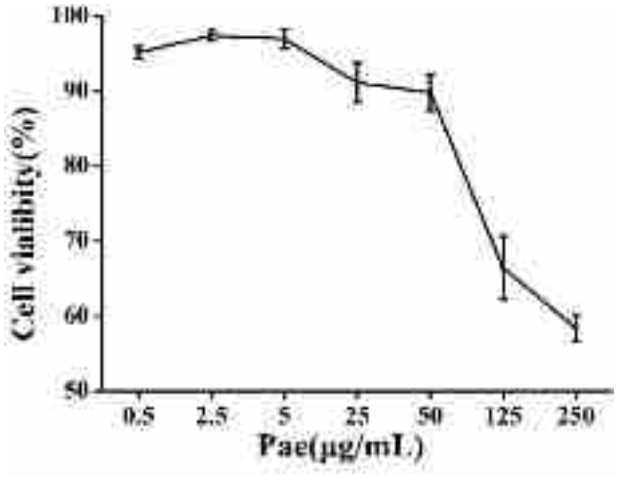

Fig. 2 Effects of Pae on the proliferation of RBL-2H3 cells (n = 3).

3.3 Pae can inhibit the release of β-Hex from RBL-2H3 cells induced by DNP-IgE/DNP-BSA and C48/80

DNP-IgE/DNP-BSA induction. The β-Hex release rate of the Model group was taken as the base. After treatment with 0.5, 2.5, and 5 μg mL^{-1} Pae, the β-Hex release rate was 55.34%, 45.77%, and 22.00%, respectively, which were significantly lower than those in the Model group ($p < 0.01$) in a dose-dependent manner. After treatment with Keto, the β-Hex release rate was 65.44% (Fig. 4A), indicating that the inhibitory effects of Pae at different concentrations were significantly stronger than those of the Keto group ($p < 0.01$).

C48/80 induction. The β-Hex release rate of the Model group was taken as the base. After treatment with 0.5, 2.5, and 5 μg mL^{-1} Pae, the β-Hex release rate was 65.24%, 27.41%, and 21.57%, respectively, which were significantly lower than those in the Model group ($P < 0.01$) in a dose-dependent manner. After treatment with Keto, the β-Hex release rate was 67.89% (Fig. 4B). The inhibitory effects of 0.5 μg mL^{-1} Pae were close to those of the Keto group, whereas the effects of 2.5 and 5 μg mL^{-1} Pae were significantly stronger than those of the Keto group ($p < 0.01$).

3.4 Pae can inhibit the release of HA from RBL-2H3 cells induced by DNP-IgE/DNP-BSA and C48/80

DNP-IgE/DNP-BSA induction. The amount of HA released in the Model group was 37.43 ng mL^{-1}, which was significantly

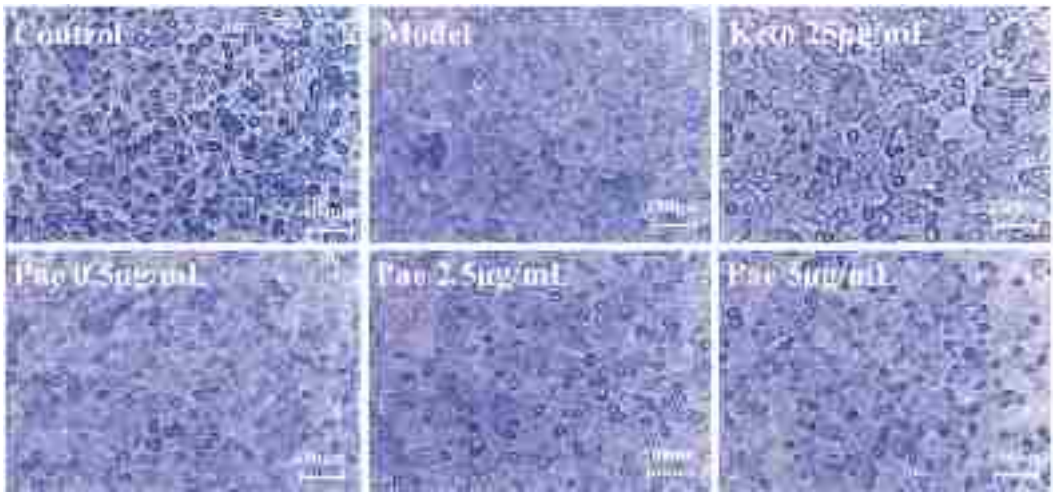

Fig. 3 Effects of Pae on the degranulation of RBL-2H3 cells by toluidine blue staining (n = 3).

This journal is © The Royal Society of Chemistry 2021

Published on 26 June 2021. Downloaded on 7/6/2021 4:12:49 AM.

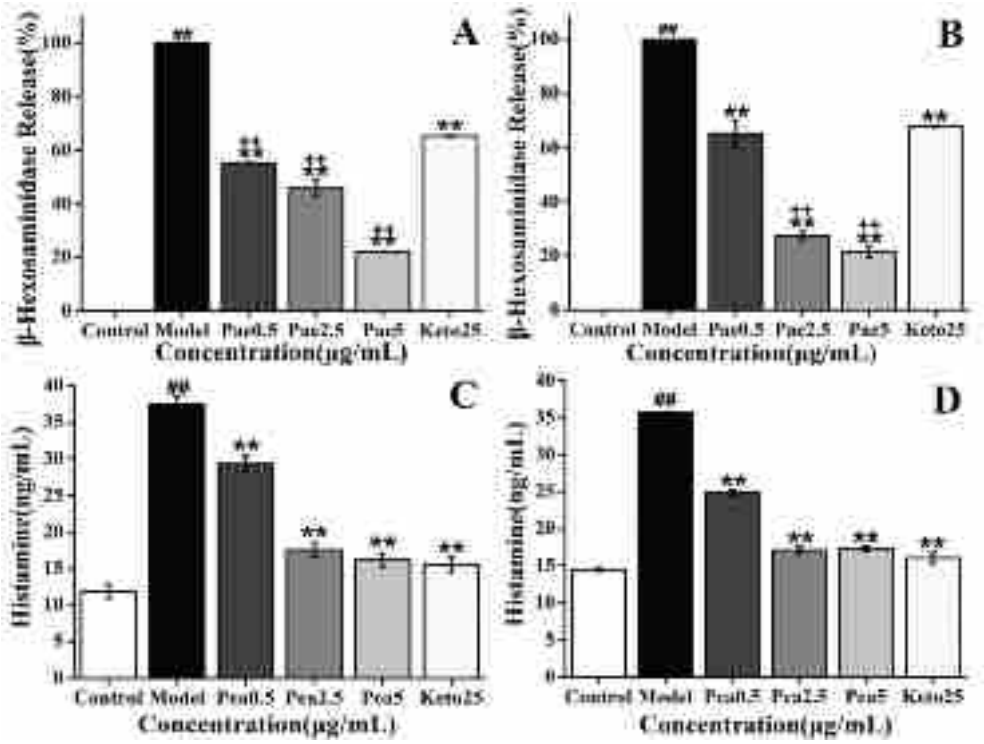

Fig. 4 Effects of Pae on the release of β-Hex and HA from RBL-2H3 cells(n = 3). (A) Induced by DNP-IgE/DNP-BSA (β-Hex); (B) induced by C48/80 (β-Hex); (C) induced by DNP-IgE/DNP-BSA (HA); (D) induced by C48/80 (HA). $^{++}p < 0.01$ *vs*. Keto; $^{**}p < 0.01$ *vs*. Model.

higher than the amount of HA released in the normal group (11.87 ng mL^{-1}, $p < 0.01$). After treatment with 0.5, 2.5, and 5 μg mL^{-1} Pae, the amount of HA released decreased to 29.3, 17.55, and 16.16 ng mL^{-1}, respectively, which were significantly lower than those in the Model group ($p < 0.01$) in a dose-dependent manner. After treatment with Keto, the amount of HA released was 15.52 ng mL^{-1} (Fig. 4C). The inhibitory effects of 2.5 and 5 μg mL^{-1} Pae were close to those of the Keto group.

C48/80 induction. The amount of HA released in the Model group was 35.67 ng mL^{-1}, which was significantly higher than that released in the normal group (14.47 ng mL^{-1}, $p < 0.01$). After treatment with 0.5, 2.5, and 5 μg mL^{-1} Pae, the amount of HA released decreased to 24.93, 17.13, and 17.33 ng mL^{-1}, which were significantly lower than those in the Model group ($p < 0.01$) in a dose-dependent manner. After treatment with Keto, the amount of HA released was 16.07 ng mL^{-1} (Fig. 4D). The inhibitory effects of 2.5 and 5 μg mL^{-1} Pae were close to those of the Keto group.

3.5 Pae can inhibit RBL-2H3 cell apoptosis induced by DNP-IgE/DNP-BSA and C48/80

DNP-IgE/DNP-BSA induction. Examination of the MCs under a fluorescence microscope revealed that the apoptosis rate of the normal group was 3.33%, and the cell structure was normal with green fluorescence. After sensitization and stimulation, the apoptosis rate significantly increased to 50.33%, which was significantly higher than that in the normal group ($p < 0.01$), and the cell structure became abnormal with green or orange fluorescence. After treatment with 0.5, 2.5, and 5 μg mL^{-1} Pae, the apoptosis rate significantly decreased to 44.33%, 37.00%, and 22.67%, respectively, which were significantly lower than those in the Model group ($p < 0.01$) in a dose-dependent manner. The apoptosis rate in the Keto group was 26.33% (Fig. 5 and 6). Treatment with 5 μg mL^{-1} Pae had a significantly stronger inhibitory effect than Keto treatment ($p < 0.01$).

C48/80 induction. The apoptosis rate of the normal group was 5.67%, and the cell structure was normal with green fluorescence. After sensitization and stimulation, the apoptosis rate significantly increased to 51.67%, which was significantly higher than that in the normal group ($p < 0.01$), and the cell structure became abnormal with green or orange fluorescence. After treatment with 0.5, 2.5, and 5 μg mL^{-1} Pae, the apoptosis rate significantly decreased to 41.00%, 34.67%, and 17.33%, respectively, which were significantly lower than those in the Model group ($p < 0.01$) in a dose-dependent manner. The apoptosis rate of the Keto group was 24.67% (Fig. 7 and 8). Treatment with 5 μg mL^{-1} Pae had a significantly stronger inhibitory effect than Keto treatment ($p < 0.01$).

3.6 Pae can reduce the Ca^{2+} concentration of RBL-2H3 cells induced by DNP-IgE/DNP-BSA and C48/80

DNP-IgE/DNP-BSA or C48/80 induction. The Ca^{2+} concentration in the normal group was extremely low. After sensitization and stimulation, Fluo-4 combined with intracellular free

Published on 26 June 2021. Downloaded on 7/6/2021 4:12:49 AM.

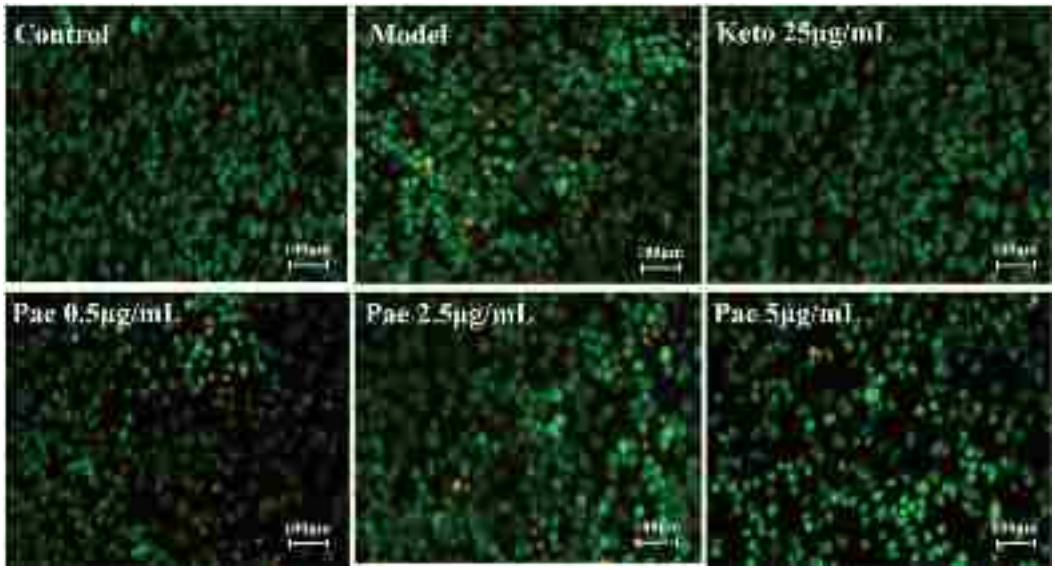

Fig. 5 Effects of Pae on apoptosis of RBL-2H3 cells induced by DNP-IgE/DNP-BSA (n = 3).

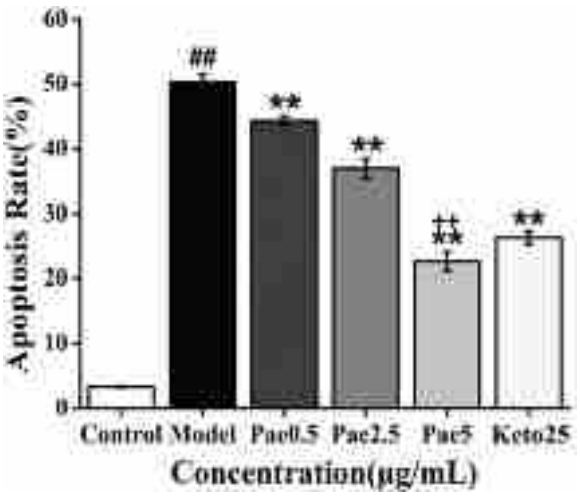

Fig. 6 Effects of Pae on apoptosis rate of RBL-2H3 cells induced by DNP-IgE/DNP-BSA (n = 3). $^{\#\#}p < 0.01$ *vs*. Control; $^{**}p < 0.01$ *vs*. Model; $^{++}p < 0.01$ *vs*. Keto.

Ca^{2+} to show green fluorescence, and the Ca^{2+} concentration substantially increased. After treatment with Pae, the concentration of Ca^{2+} considerably decreased in a dose-dependent manner (Fig. 9 and 10). The concentration of Ca^{2+} was close after treatment with 5 μg mL^{-1} Pae and Keto.

3.7 Pae can inhibit the phosphorylation of Lyn and Syk proteins during RBL-2H3 cell degranulation induced by DNP-IgE/DNP-BSA

As shown in Fig. 11, the phosphorylation levels of Lyn and Syk in the normal group were extremely low. After sensitization and stimulation, the phosphorylation levels significantly increased and was significantly higher than those in the normal group ($p < 0.01$). After treatment with 0.5, 2.5, and 5 μg mL^{-1} Pae, the phosphorylation levels of Lyn and Syk decreased in a dose-dependent manner. Compared with the Model group, treatment with 2.5 and 5 μg mL^{-1} Pae had significant differences ($p < 0.01$). The phosphorylation levels of Lyn and Syk remarkably decreased after Keto treatment. The inhibitory effects of 5 μg mL^{-1} Pae on the phosphorylation level of Lyn was similar to that in the Keto group.

3.8 Effects of Pae on gene expression during RBL-2H3 cell degranulation induced by DNP-IgE/DNP-BSA

3.8.1 Pae can inhibit the expression of Lyn, Syk, Fyn and PLCγ genes in the IgE signaling pathway. qPCR revealed that Pae inhibited the expression levels of the Lyn, Syk, Fyn, and PLCγ genes during the degranulation of RBL-2H3 cells induced by DNP-IgE/DNP-BSA in a dose-dependent manner (Fig. 12). The inhibitory effects of 5 μg mL^{-1} Pae on Syk, Fyn, and PLCγ were stronger than those of the Keto group.

3.8.2 Pae can inhibit the expression of the key genes in the PI3K/Akt, MAPK, and NF-κB signaling pathways. Results showed that Pae inhibited the expression levels of the PI3K, Akt, ERK, JNK, p38, and p65 genes during the degranulation of RBL-2H3 cells induced by DNP-IgE/DNP-BSA. Except for Akt and ERK, the inhibition of the genes' expression levels occurred in a dose-dependent manner (Fig. 13). The inhibitory effects of 5 μg mL^{-1} Pae on ERK, p38, and p65 were stronger than those of the Keto group.

3.8.3 Pae can inhibit the expression of ORAI-1 and ORAI-2. Pae inhibited the expression levels of the ORAI-1 and ORAI-2 genes during the degranulation of RBL-2H3 cells induced by DNP-IgE/DNP-BSA in a dose-dependent manner (Fig. 14A and B).

3.8.4 Effects of Pae on the expression of IFN-γ and IL-4. Pae inhibited the expression of the IL-4 gene during the degra-

 This journal is © The Royal Society of Chemistry 2021

Published on 26 June 2021. Downloaded on 7/6/2021 4:12:49 AM.

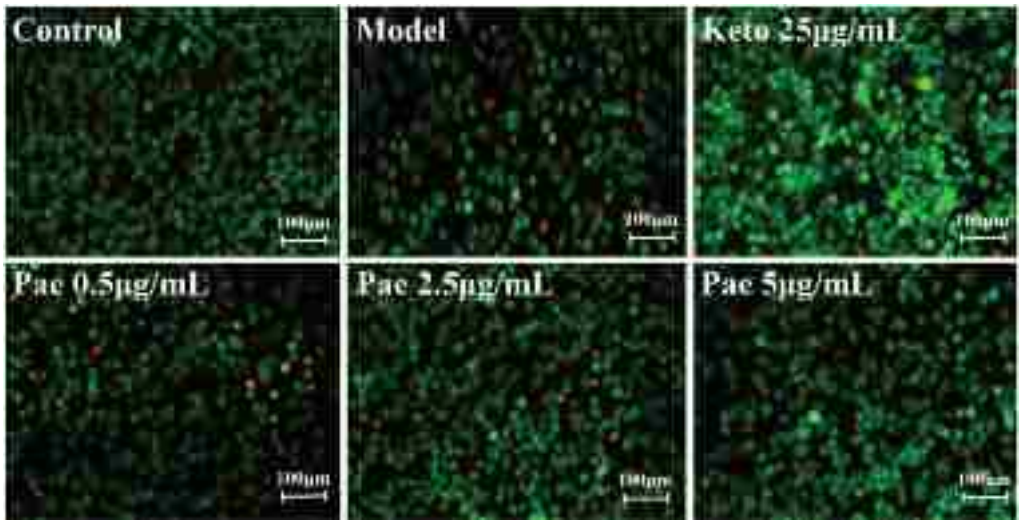

Fig. 7 Effects of Pae on apoptosis of RBL-2H3 cells induced by C48/80 (n = 3).

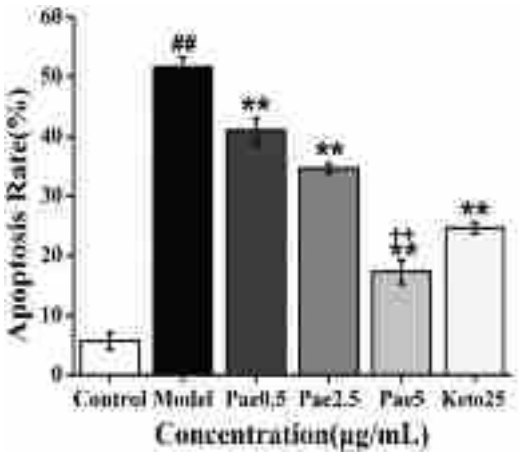

Fig. 8 Effects of Pae on apoptosis rate of RBL-2H3 cells induced by C48/80 (n = 3). $^{\#\#}p < 0.01$ *vs*. Control; $^{**}p < 0.01$ *vs*. Model; $^{++}p < 0.01$ *vs*. Keto.

nulation of RBL-2H3 cells induced by DNP-IgE/DNP-BSA in a dose-dependent manner. The inhibitory effects of 2.5 and 5 μg mL^{-1} Pae were substantially stronger than those of the Keto group. However, the inhibitory effects of Pae on the expression of the IFN-γ gene was not obvious, and only 5 μg mL^{-1} Pae had a certain inhibitory effect (Fig. 14C and D).

3.9 Pae can inhibit the PCA of mice induced by DNP-IgE/DNP-BSA and C48/80

3.9.1 PCA of the ear

DNP-IgE/DNP-BSA or C48/80 induction. As shown in Fig. 15 and 16, no Evans Blue extravasation appeared in the ears of the mice in the normal group. By contrast, the Model group had the highest Evans Blue extravasation. After treatment with Pae, the content of Evans Blue decreased in a dose-dependent manner, which was significantly lower than that of the Model group ($p < 0.01$). The inhibitory effects of 100 mg kg^{-1} Pae were significantly stronger than those of the Keto group ($p < 0.01$).

The results of ear swelling test showed that the swelling decreased after treatment with Pae in a dose-dependent manner, which was significantly lower than that of the Model group ($p < 0.01$). The inhibitory effects of 50 and 100 mg kg^{-1} Pae were significantly stronger than those of the Keto group ($p < 0.01$).

3.9.2 PCA of the paw

DNP-IgE/DNP-BSA or C48/80 induction. As shown in Fig. 17 and 18, no Evans Blue extravasation appeared in the paws of the mice in the normal group. By contrast, the Model group had the highest Evans Blue extravasation. After treatment with Pae, the content of Evans Blue decreased in a dose-dependent manner, which was significantly lower than that of the Model group ($p < 0.05$ or $p < 0.01$). The inhibitory effects of 100 mg kg^{-1} Pae were close to those of the Keto group.

The results of paw swelling test showed that the swelling decreased after treatment with Pae in a dose-dependent manner, which was significantly lower than that of the Model group ($p < 0.01$). The inhibitory effects of 100 mg kg^{-1} Pae were close to those of the Keto group.

3.9.3 PCA of the back skin

DNP-IgE/DNP-BSA or C48/80 induction. As shown in Fig. 19 and 20, no Evans Blue extravasation was observed on the back skin of the mice in the normal group. By contrast, a large area of Evans Blue extravasation appeared on the back skin of the Model group. After treatment with Pae, the diameter and content of Evans Blue extravasation decreased in a dose-dependent manner, which was significantly lower than that of the Model group ($p < 0.01$). The inhibitory effects of 100 mg kg^{-1} Pae were significantly stronger than those of the Keto group ($p < 0.01$).

Published on 26 June 2021. Downloaded on 7/6/2021 4:12:49 AM.

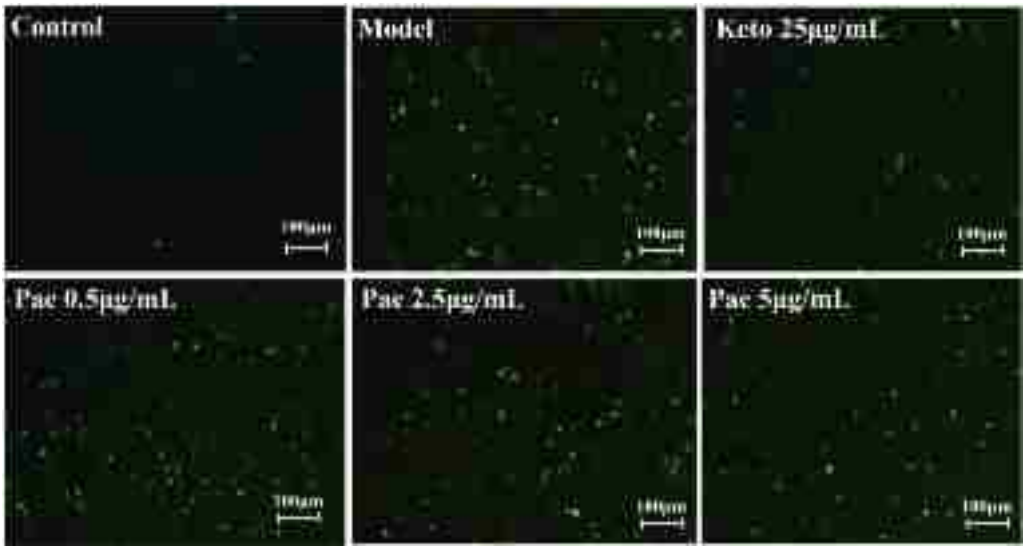

Fig. 9 Effects of Pae on the Ca^{2+} concentration of RBL-2H3 cells induced by DNP-IgE/DNP-BSA (n = 3).

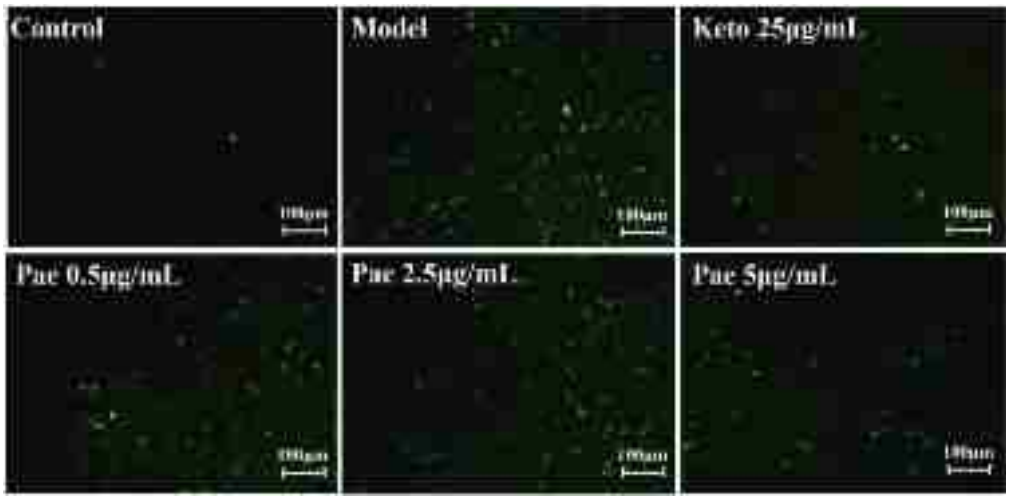

Fig. 10 Effects of Pae on the Ca^{2+} concentration of RBL-2H3 cells induced by C48/80 (n = 3).

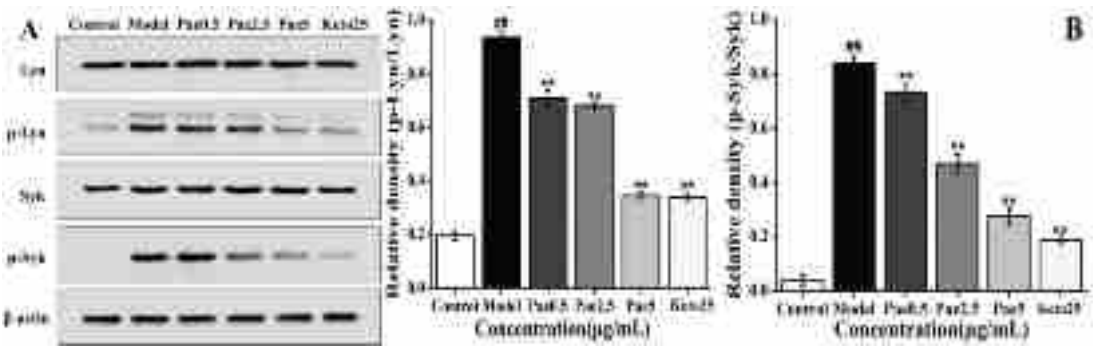

Fig. 11 Effects of Pae on the phosphorylation of Lyn and Syk proteins (n = 3). (A) Western blot detects the phosphorylation of Lyn and Syk proteins in RBL-2H3 cells induced by DNP-IgE/DNP-BSA. (B) Results of density analysis. $^{\#\#}p < 0.01$ *vs*. control; $^{**}p < 0.01$ *vs*. Model.

This journal is © The Royal Society of Chemistry 2021

Published on 26 June 2021. Downloaded on 7/6/2021 4:12:49 AM.

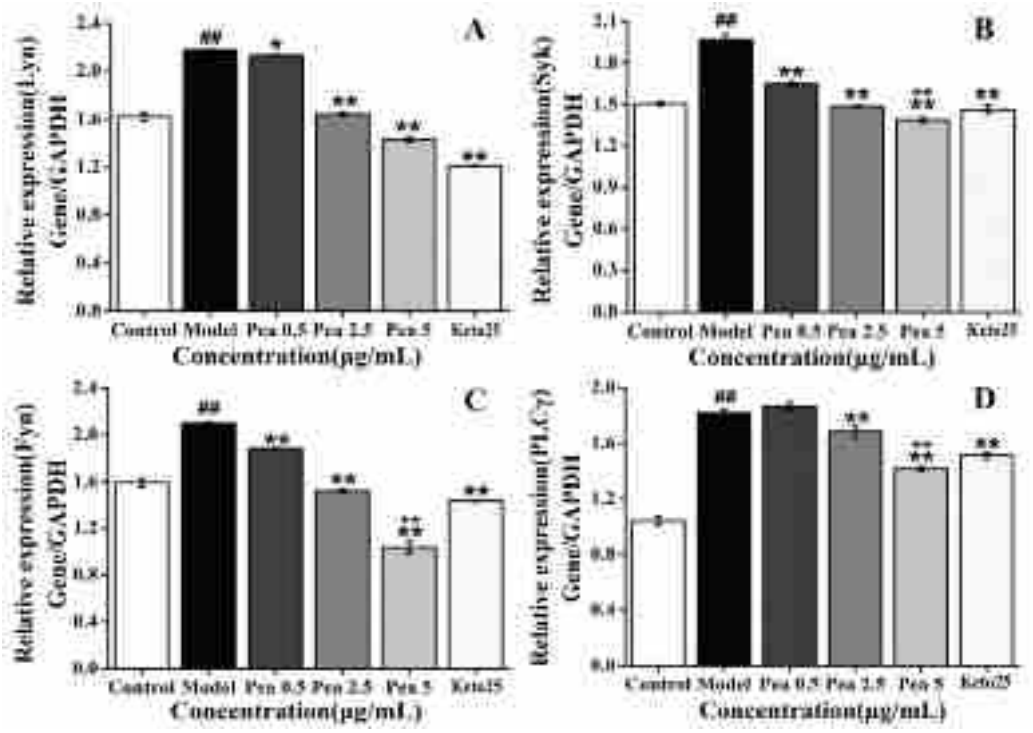

Fig. 12 Effects of Pae on the expression of Lyn, Syk, Fyn and PLCγ genes in the IgE signaling pathway (n = 3). (A) Lyn; (B) Syk; (C) Fyn; (D)PLCγ. $^{\#\#}p < 0.01$ *vs*. control; $^{*}p < 0.05$, $^{**}p < 0.01$ *vs*. Model; $^{++}p < 0.01$ *vs*. Keto.

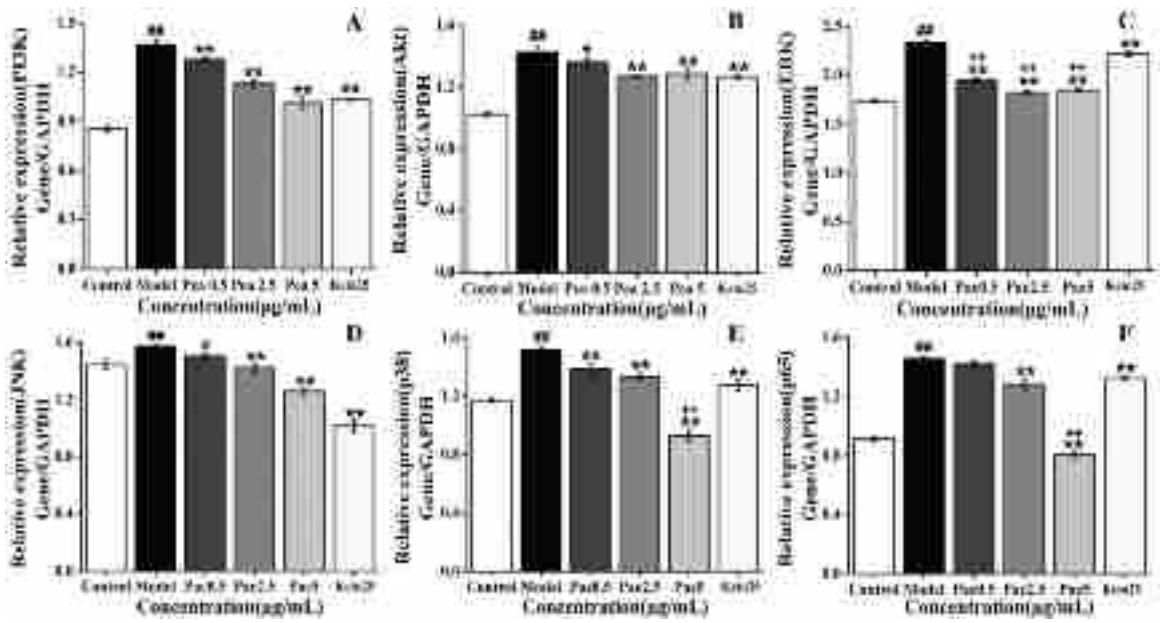

Fig. 13 Effects of Pae on the expression of PI3K, Akt, ERK, JNK, p38 and p65 genes (n = 3). (A) PI3K; (B) Akt; (C) ERK; (D) JNK; (E) p38; (F) p65. $^{\#\#}p < 0.01$ *vs*. control; $^{*}p < 0.05$, $^{**}p < 0.01$ *vs*. Model; $^{++}p < 0.01$ *vs*. Keto.

4. Discussion

Paeoniae Radix Rubra is an edible Chinese medicine with health benefits and therapeutic effects. Its immunomodulation and anti-inflammatory effects are mainly attributed to Pae; hence, this compound has been widely studied. Pae can reportedly protect the liver; has anti-inflammatory, immunomodulation, and antitumor effects; can promote angiogenesis

Published on 26 June 2021. Downloaded on 7/6/2021 4:12:49 AM.

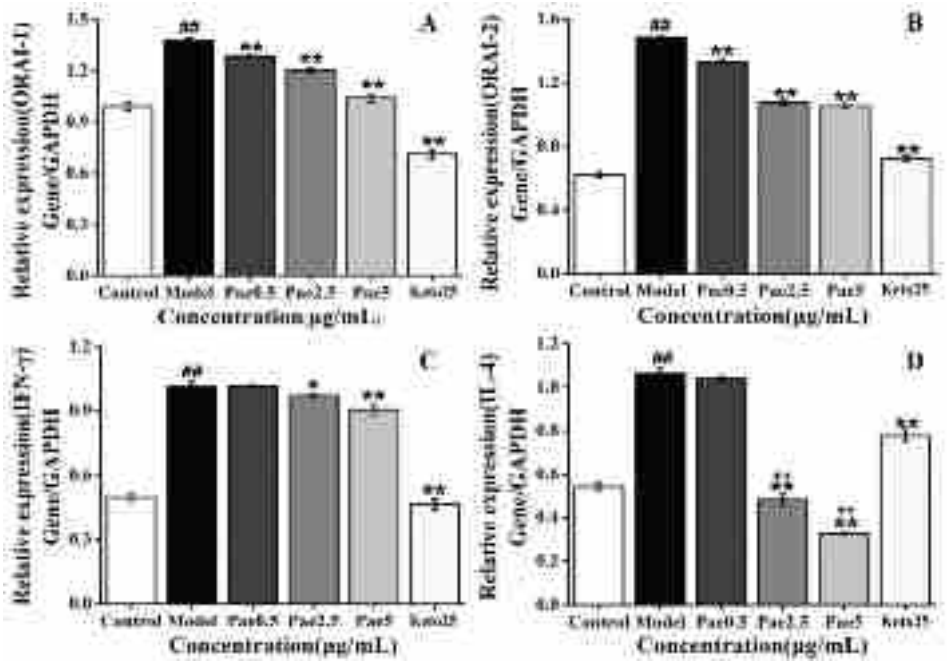

Fig. 14 Effects of Pae on the expression of ORAI-1, ORAI-2, IFN-γ and IL-4 genes (n = 3). (A) ORAI-1; (B) ORAI-2; (C) IFN-γ; (D) IL-4. $^{\#\#}p < 0.01$ *vs*. control; $^{*}p < 0.05$, $^{**}p < 0.01$ *vs*. Model; $^{++}p < 0.01$ *vs*. Keto.

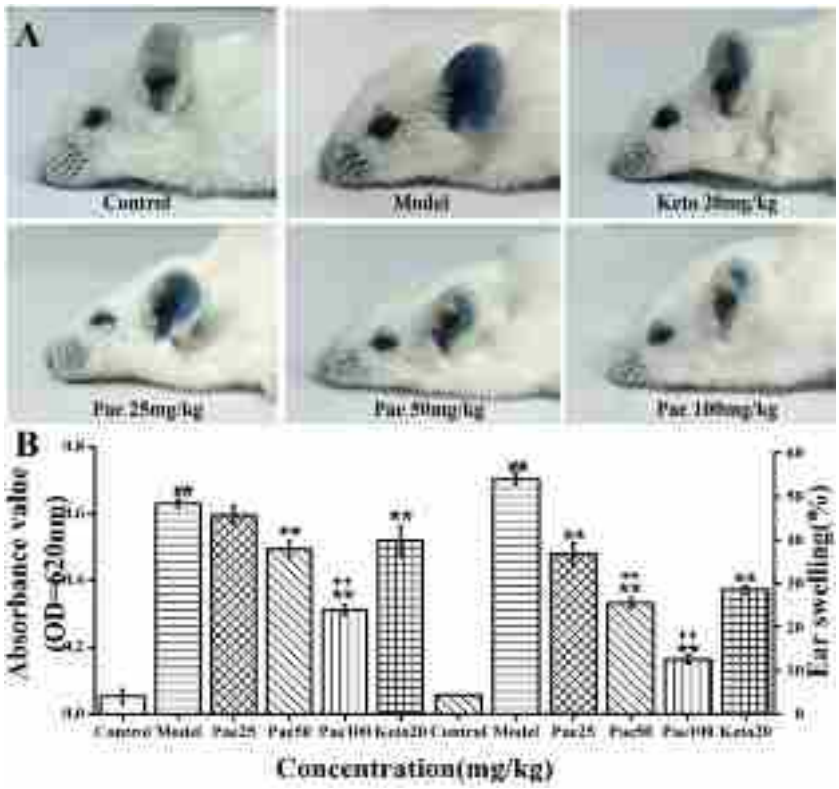

Fig. 15 Effects of Pae on Evans Blue extravasation and swelling in mouse ears induced by IgE (n = 6). (A) Evans blue extravasation in the ears; (B) Evans blue content and swelling of ears.

This journal is © The Royal Society of Chemistry 2021

Published on 26 June 2021. Downloaded on 7/6/2021 4:12:49 AM.

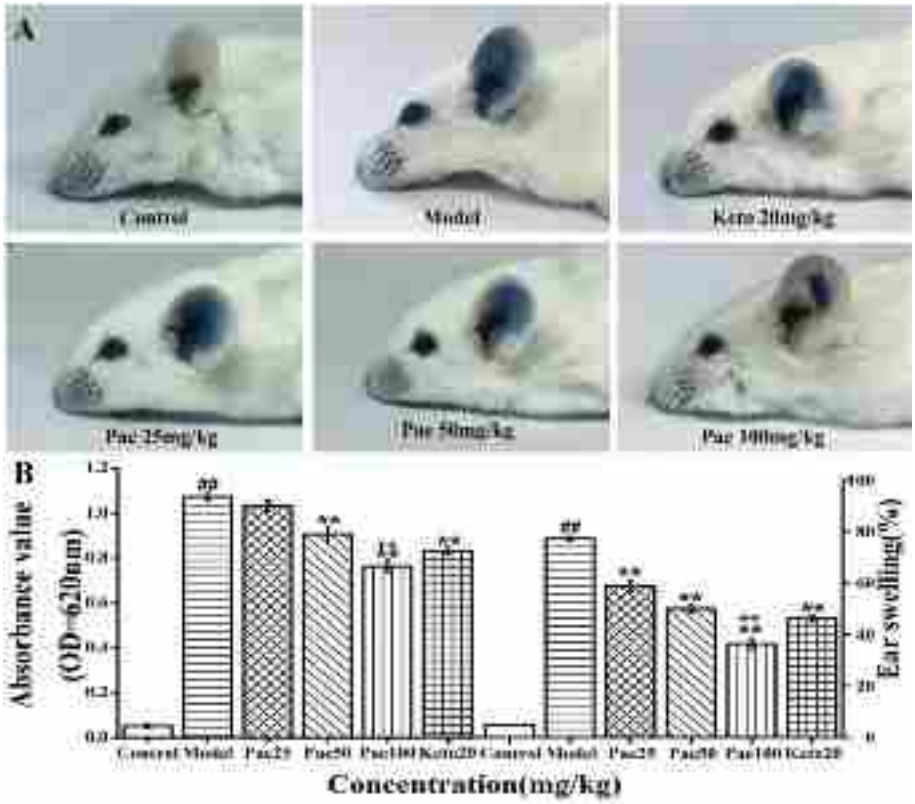

Fig. 16 Effects of Pae on Evans Blue extravasation and swelling in mouse ears induced by C48/80 (n = 6). (A) Evans blue extravasation in the ears; (B) Evans blue content and swelling of ears. $^{\#\#}p < 0.01$ *vs*. Control; $^{**}p < 0.01$ *vs*. Model; $^{++}p < 0.01$ *vs*. Keto.

and tissue regeneration; and has good clinical treatment effects on neurological diseases, such as Alzheimer's disease, depression, and epilepsy.[9,10] In addition, Pae is closely related to the PI3K/Akt, NF-κB, and MAPK pathways, as well as other signaling pathways associated with allergic reactions. Moreover, Pae can regulate the balance of Th1/Th2. Thus, Pae can be potentially used as a drug for the treatment of allergic reactions. Previous studies on the mechanism by which Pae inhibits MC degranulation have been conducted, but they all have limitations, and the relevant mechanism has not been sufficiently investigated. Therefore, the inhibitory effects and the mechanism by which Pae acts on allergies must be comprehensively evaluated.[12–14]

MCs are the main response cells regardless if the disease is type I allergies or pseudoallergic reactions. The stimuli that induce MCs degranulation can be divided into two categories: immune stimuli and nonimmune stimuli. Immune stimuli mainly include IgE, which degranulates MCs by binding to the high-affinity receptor (FcεR I). DNP-IgE/DNP-BSA is a commonly used sensitizer and stimulator that activates the IgE signaling pathway to induce MCs degranulation.[15] IgE contains the Fc region, which can bind to FcεR I on the surface of MCs to sensitize the body. When stimulated by the corresponding antigen again, the antigen can bind to IgE on the surface of the sensitized MCs and cause cross-linking FcεR I activation and ITAM phosphorylation, both of which further activate the tyrosine kinase and downstream signaling pathways, leading to MCs degranulation.

Nonimmune stimuli, such as Ca^{2+} ionophores, C48/80, and neuropeptides (substance P), can activate MCs. The Mas-related G protein coupled receptor X (MRGPRX) may be the receptor for nonimmune stimuli to activate MCs. This MRGPRX family has only four genes in humans: MrgX1-X4. McNeil[16] found that the homologous gene of MRGPRX2 is MRGPRB2 in the MCs of mice, and MRGPRB2 is a specific molecule on MC membrane surface. Thus, it can be considered as the receptor for secretagogue and many drugs that cause pseudoallergic reactions. This feature makes the receptor a drug target. The preparation of small-molecule compounds that block MRGPRX2 in humans can inhibit the allergic reactions caused by various drugs. Nonimmune stimuli can activate the G protein and continue to transmit signals through its subunits α, β, and γ, eventually triggering MCs degranulation.[17] Another possibility is that it activates phospholipase γ (PLCγ) directly or indirectly, thereby activating protein kinase C and opening the intracellular Ca^{2+} storehouse, both of which also trigger MCs degranulation.[18–20] C48/80 is a synthetic polyamine compound produced by the condensation of formaldehyde and *N*-methyl-*p*-methoxyphenethylamine. It is commonly used to stimulate MCs to produce allergic mediators.[21] It can release HA and other biologically active mediators by binding to MRGPRX2 on the surface of basophils

Published on 26 June 2021. Downloaded on 7/6/2021 4:12:49 AM.

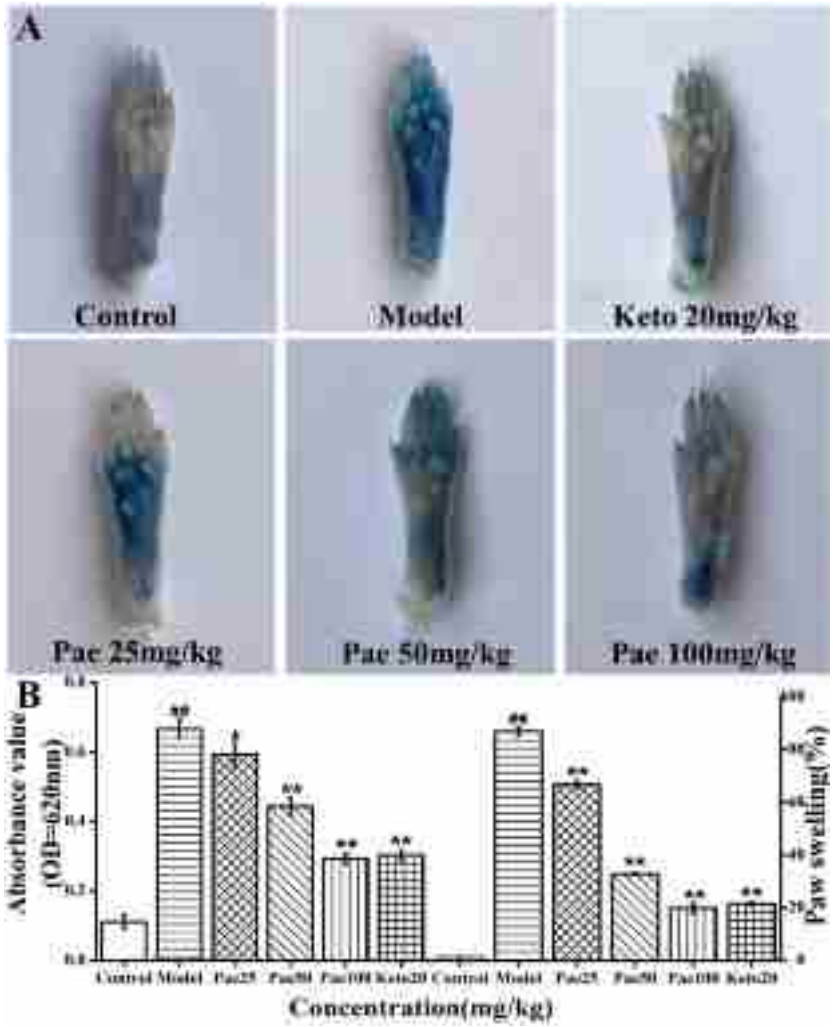

Fig. 17 Effects of Pae on Evans Blue extravasationand swelling in mouse paws induced by IgE (n = 6). (A) Evans blue extravasation in the paws; (B) Evans blue content and swelling of paws. $^{\#\#}p < 0.01$ *vs*. Control; $^{*}p < 0.05$, $^{**}p < 0.01$ *vs*. Model.

or MCs. This process is related to the pseudoallergic reactions caused by drugs. In previous studies, C48/80 and PMACI were used as stimulators to evaluate the inhibitory effects of Pae on MCs degranulation. However, the mechanism is different from that of IgE/FcεR I, and it can only simulate cell degranulation in pseudoallergic reactions.[22,23] Therefore, in our study, the two induction methods of DNP-IgE/DNP-BSA and C48/80 were adopted to establish the model of MCs degranulation and comprehensively explore the therapeutic effects of Pae on type I allergies and pseudoallergic reactions.

RBL-2H3 cells possess the biological characteristics of MCs. Thus, RBL-2H3 cells are used as the classic model for studying degranulation reaction *in vitro*.[24] Yu *et al.*[22] and Wang *et al.*[23] adopted P815 and HMC-1 cells as *in vitro* models to assess the inhibitory effects of Pae on MCs degranulation. However, the content of IgE high-affinity receptor (Fcthe) in these two cells was extremely low, and type I allergies were mediated by IgE. Therefore, the role of Pae in the activated MCs line RBL-2H3 cells (containing numerous Fcmerouswas not elucidated. Zhang *et al.*[12] and Wang *et al.*[13] chose LAD2 cells (human MCs). Although mouse IgE can bind to human MCs, species-specific interference can interfere with the degree of MCs degranulation. Therefore, after considering various factors, we finally chose RBL-2H3 cells as the cell model. The most common method used in detecting degranulation involves detecting changes in morphology, measuring the release of HA and β-Hex, monitoring changes in Ca^{2+} concentration, and detecting cell apoptosis. To improve the reliability of the results, we chose Keto as the positive control drug. It is the histamine H1 receptor antagonist and has a strong anti-allergic effect. It can inhibit the release of allergic mediators from MCs and stabilize their membranes. Keto can also block Ca^{2+} channels and inhibit IgE synthesis. Thus, it is often used as a positive control drug in anti-allergy experiments.[25]

Mature MCs are round or oval, and their cytoplasm is filled with particles that can be dyed blue-purple by toluidine blue, such as heparin and HA. When MCs degranulation occurs, the morphology of cells becomes irregular and particles are

 This journal is © The Royal Society of Chemistry 2021

Published on 26 June 2021. Downloaded on 7/6/2021 4:12:49 AM.

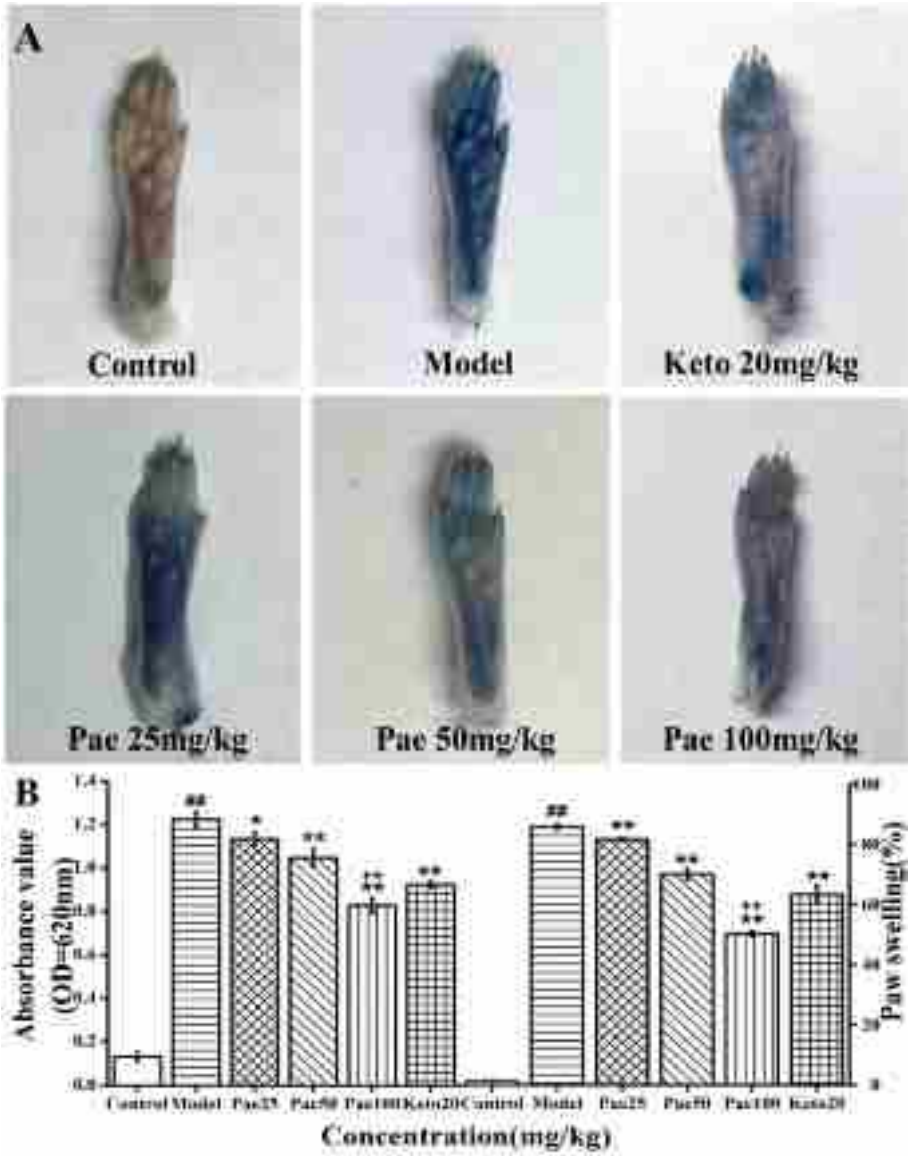

Fig. 18 Effects of Pae on Evans Blue extravasation and swelling in mouse paws induced by C48/80 (n = 6). (A) Evans blue extravasation in the paws; (B) Evans blue content and swelling of paws. $^{\#\#}p < 0.01$ *vs*. Control; $^{*}p < 0.05$, $^{**}p < 0.01$ *vs*. Model; $^{++}p < 0.01$ *vs*. Keto.

released, which can cause immediate allergic reactions.[26] The results of the present study demonstrated that Pae can inhibit morphological changes in RBL-2H3 cells during degranulation.

β-Hex content substantially increases only when the body is in an allergic state. Only MCs can release β-Hex, and it is often accompanied with the release of HA; thus, it is usually used as a marker of MCs degranulation.[27,28] HA has a strong vasodilatory effect and can increase vascular permeability, thereby causing swelling of local tissues, which can cause allergic reactions. Therefore, HA is also a marker of MCs degranulation.[29,30] In this experiment, Pae was found to inhibit the degranulation of RBL-2H3 cells induced by DNP-IgE/DNP-BSA and C48/80 and considerably reduce the release of HA and β-Hex in a dose-dependent manner.

The key factor that triggers MCs degranulation is the increase in intracellular Ca^{2+} concentration.[31] The degranulation induced by immune stimuli depends on the influx of extracellular Ca^{2+} into cells, a situation that increases intracellular Ca^{2+} concentration. Simulatneously, inositol triphosphate can also be generated to release the Ca^{2+} stored in the endoplasmic reticulum, thereby increasing the level of intracellular Ca^{2+}.[32] C48/80, a nonimmune stimuli, can act on the MCs membrane and promote large amounts of Ca^{2+} to flow into cells from the outside, thereby causing MCs degranulation and releasing large amounts of HA.[33] Therefore, the concentration of Ca^{2+} is often widely used as a classic indicator of MCs degranulation. Fluo-4,AM is a fluorescent probe that can penetrate cell membranes. It is commonly employed to detect the concentration of intracellular

Published on 26 June 2021. Downloaded on 7/6/2021 4:12:49 AM.

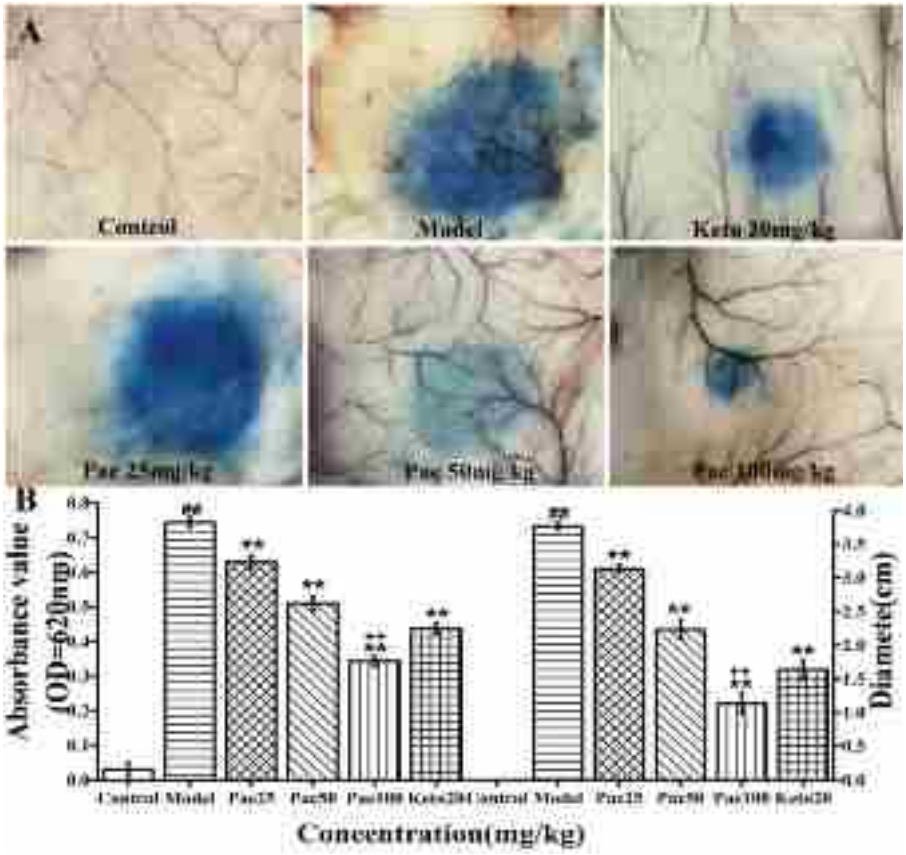

Fig. 19 Effects of Pae on Evans Blue extravasation and diameter in mouse back skin induced by IgE (n = 6). (A) Evans blue extravasation in the back skin; (B) Evans blue content and diameter of back skin. $^{\#\#}p < 0.01$ *vs*. Control; $^{**}p < 0.01$ *vs*. Model; $^{++}p < 0.01$ *vs*. Keto.

Ca^{2+}. The results of Fluo-4,AM staining showed that Ca^{2+} concentration substantially increased after DNP-IgE/DNP-BSA and C48/80 were used. After Pae treatment, the concentration of intracellular Ca^{2+} tended to decrease, suggesting that Pae may inhibit the release of HA and β-Hex by regulating the Ca^{2+} concentration in MCs.

Pae can regulate the classic signalling pathways, such as MAPK and PI3K/Akt, during the treatment of inflammation and cancer; moreover, Pae can regulate cell proliferation and apoptosis by regulating the activity of NF-κB.[34–36] In this study, Pae was observed to inhibit RBL-2H3 cells apoptosis induced by DNP-IgE/DNP-BSA and C48/80 to varying degrees. Subsequent qPCR experiments suggested that Pae may affect the PI3K/Akt, MAPK, and NF-κB signaling pathways by inhibiting the expression of the PI3K, Akt, ERK, JNK, p38, and p65 genes. These signaling pathways ultimately inhibit RBL-2H3 cells apoptosis through extensive connections and effects. Most previous reports on the relationship between Pae and allergy only focused on showing the inhibitory effects of this compound and lacked in-depth exploration of the underlying mechanism.[12–14] However, the pathogenesis of allergy is extremely complex, and more signaling pathways and molecular mechanisms must be explored. To address these limitations, we combined the results reported in the literature and conducted our own experiments to comprehensively analyze the underlying mechanism. IgE/FcεR I is a classic signaling pathway that directly regulates type I allergies. It includes non-receptor tyrosine kinases, such as Syk, Lyn, and Fyn. Lyn and Syk participate in the activation of MCs as the initial signals of the IgE/FcεR I signaling pathway, and they are the key therapeutic targets for allergic diseases.[37] Syk can amplify downstream cell signals, and activated Syk can further activate certain adaptor proteins, such as LAT, thereby activating PLCγ and PI3K.[38] The lack of LAT in MCs reportedly affects Ca^{2+} signal transduction, and MCs degranulation can be inhibited by preventing the activation of PLCγ.[39] Recent studies showed that Fyn also plays an important role in MCs degranulation and is upstream of this signaling pathway.[40] The cross-linking of FcεR I can also activate Gab2 on which Fyn depends, and Gab2 can bind to PI3K. PI3K can then catalyze the synthesis on the membrane of phosphatidylinositol (3,4,5)-bisphosphate (PIP3), which is very important for the release of Ca^{2+}.[41] PIP3 is an activator of phosphoinositide-dependent kinase 1 (PDK1), and Akt can be activated by PDK1. This study found that Pae inhibited the phosphorylation of the Lyn and Syk proteins and the expression levels of the Lyn, Syk, Fyn, PLCγ, PI3K, and Akt genes during MCs degranulation, suggesting that Pae can inhibit the IgE/FcεR I and PI3K/Akt signaling

 This journal is © The Royal Society of Chemistry 2021

Published on 26 June 2021. Downloaded on 7/6/2021 4:12:49 AM.

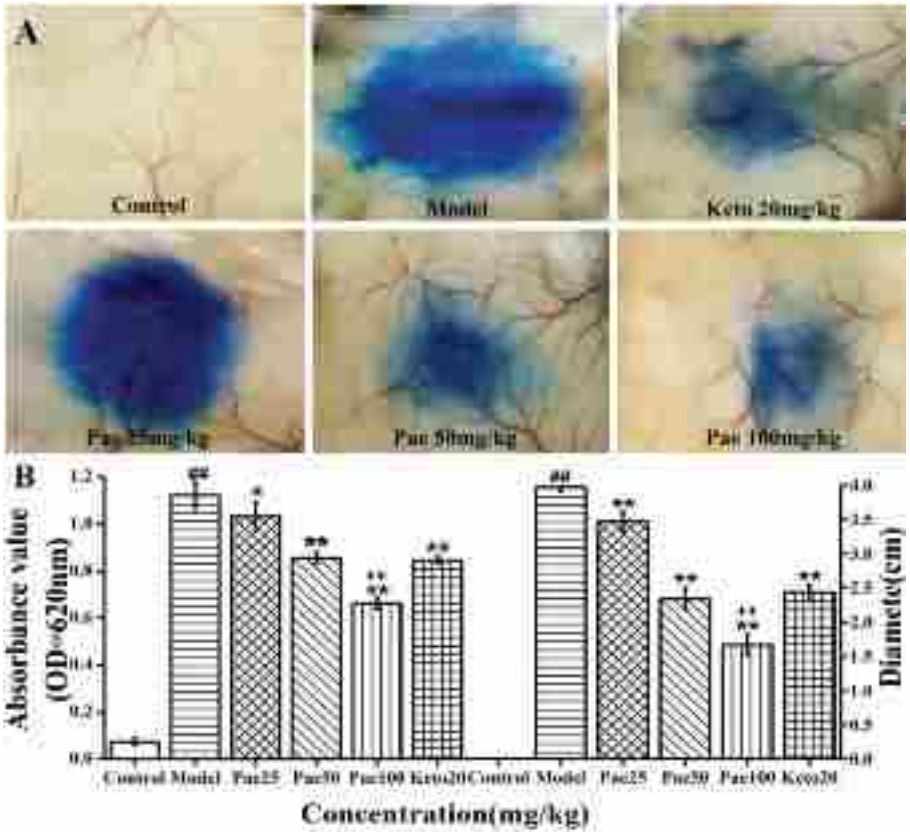

Fig. 20 Effects of Pae on Evans Blue extravasation content and diameter in mouse back skin induced by C48/80 (n = 6). (A) Evans blue extravasation in the back skin; (B) Evans blue content and diameter of back skin. $^{\#\#}p < 0.01$ *vs*. Control; $^{*}p < 0.05$, $^{**}p < 0.01$ *vs*. Model; $^{++}p < 0.01$ *vs*. Keto.

pathways. We speculated that this inhibitory effect may depend on changes in Ca^{2+} concentration.

The Lyn-Syk kinase-dependent signaling pathway can directly or indirectly activate the downstream classic signaling pathways, such as MAPK and NF-κB.[42] The MAPK cascade is an important signaling pathway that regulates the immune reaction, and it also regulates inflammation through close contact with NF-κB.[43] MAPK is a group of serine/threonine protein kinases that can be activated by Ras, which is mainly composed of three subunits, namely, JNK, ERK, and p38.[44] They mediate extracellular and nuclear signal transduction, promote MCs to secrete biologically active mediators, and combine growth factors and cytokines to participate in allergic reactions.[45,46] NF-κB is a dimeric nuclear transcription factor formed by heterologous or homologous proteins p50 and p65 in the Rel family, and it plays an important role in immune and inflammatory reactions.[47] Kee[48,49] found that ginsenoside Rg3 and the water extract of red ginseng can regulate the expression of pro-inflammatory factors and chemokines through the MAPK and NF-κB signaling pathways, thereby inhibiting the occurrence of allergic reactions. Li[50] revealed that cornus can inhibit allergic reactions by downregulating the MAPK and NF-κB signaling pathways. Wang *et al.*[23] reported that Pae inhibits the activation of MCs by suppressing the NF- of thways. Allergiing pathways from the perspective of anti-inflammatory effects. Yu *et al.*[22] only clarified the inhibitory effects of Pae on MCs activation by blocking the PI3K/AKT/m-TOR signal pathway. Owing to the complexity of cell signal networks involved in allergy, these results should only be a part of the mechanism that plays a role in inhibition. The results of qPCR in our study demonstrated that Pae can substantially inhibit the expression of the JNK, p38, and p65 genes during the degranulation of RBL-2H3 cells. However, the inhibitory effects on the expression of the ERK gene was relatively weak, indicating that the inhibitory effects of Pae may be selective. In summary, Pae exerted an inhibitory effect on the key downstream genes of the IgE/FcεR I signaling pathway, indicating that Pae has multidimensional regulatory mechanism on allergic reactions.

The imbalance of Th1/Th2 in the body and the predominance of Th2 cells are important characteristics of allergic reactions.[51,52] IgE is a key factor in the occurrence of type I allergies, and its synthesis is regulated by IL-4 and IFN-γ. IL-4 is derived from Th2 cells and MCs, both of which can increase the content of IgE in the body and eventually lead to allergic reactions.[53,54] IFN-γ, which is derived from Th1 cells, is related to the degree of inflammation, and it can inhibit the functions of IgE.[55,56] Chuang[57] showed that when the body has allergic symptoms, such as allergic asthma and allergic rhinitis, the level of IL-4 substantially increases but the level of IFN-γ

Published on 26 June 2021. Downloaded on 7/6/2021 4:12:49 AM.

decreases. The results of this study showed that Pae considerably inhibited the expression of IL-4 but had almost no effect on IFN-γ expression. Therefore, Pae probably inhibited degranulation by reducing the ratio of IL-4 to IFN-γ, thereby regulating the Th1/Th2 balance. In addition, although the mechanism by which Pae regulates the Th1/Th2 balance was different from that by Keto, both of them inhibited MCs degranulation.

C48/80 can combine with MRGPRX2 and MRGPRB3 (the rat homologous gene of human MRGPRX2) to induce MCs degranulation.[58,59] MRGPRX2 can be specifically expressed on the surface and plasma membrane of MCs.[60] When MRGPRX2 is stimulated, the influx of Ca^{2+} is the first response of MCs.[61] MRGPRX2 expressed on the surface and plasma membrane of MCs may participate in MCs degranulation through Ca^{2+} channels regulated by Ca^{2+} release-activated calcium channel protein 1 (ORAI-1) and ORAI-2, respectively, and will eventually trigger pseudoallergic reactions. The results of this study showed that Pae notably inhibited the expression levels of ORAI-1 and ORAI-2, and the inhibitory effects on the two genes were similar. Therefore, Pae possibly inhibited the pseudoallergic reactions caused by the MRGPRB3 signaling pathway by affecting the changes in Ca^{2+}. However, research on the MRGPRX2 signaling pathway is still ongoing. Thus, the specific regulation process of Pae must be explored in depth.

PCA, which was first established by Ovary,[62,63] is often used to evaluate the therapeutic effects of drugs on IgE-mediated allergic reactions. This method is simple to operate and has a high sensitivity and specificity. PCA is caused by allergens to stimulate the body to increase vascular permeability and cause swelling of local tissues, leading to allergic reactions of local skin.[64] Although many factors affect the results of PCA, such as dose, frequency and route of sensitization, and animal species, the PCA model is a classic animal model for evaluating the anti-allergic activity of drugs. Early studies that established the PCA model confirmed that Keto has anti-allergic activity.[65]

According to different mechanisms of cell degranulation, two induction methods, namely, DNP-IgE/DNP-BSA and C48/80, were used to establish PCA models of the ear, paw and back skin of mice. Zhang *et al.*[12] established the model by one-time injection of OVA, which is not consistent with the clinical pathogenesis of allergy. As a result, this method is not widely used. Zhang *et al.*[12] only analyzed the PCA conditions of the paw of mice. Our results showed obvious Evans Blue extravasation in the sensitized area of the Model group; this group had the widest range, the darkest color, and the highest degree of swelling, indicating that the local skin of the mice had allergic reactions. Compared with the Model group, the diameter of Evans Blue extravasation in the corresponding part of the Pae group decreased, the color became lighter, the degree of swelling decreased, and the dosage of Pae was positively correlated with the anti-allergic effects. In addition, Pae had a strong inhibitory effect on the two PCA models induced by DNP-IgE/DNP-BSA and C48/80, further proving that Pae has an anti-allergic activity.

5. Conclusion

This study confirmed that Pae has therapeutic effects on type I allergies and pseudoallergic reactions both *in vitro* and *in vivo* through cell and animal models, respectively. Pae may regulate the IgE/FcεR I and MRGPRB3 signaling pathways, as well as downstream signaling pathways, and regulate the body's Th1/Th2 balance, thereby exerting its therapeutic effects. Our findings suggested that Pae has the potential as a therapeutic drug for preventing or treating IgE-dependent and IgE-independent allergic diseases. There is no doubt that in order to fully reveal the mechanism of Pae, further in-depth research is needed.

Abbreviation

IgE	Immunoglobulin E
MC	Mast cells
HA	Histamine
β-Hex	β-Hexosaminidase
5-HT	5-Hydroxytryptamine
C48/80	Compound 48/80
Pae	Paeoniflorin
PCA	Passive cutaneous anaphylaxis
Keto	Ketotifen fumarate
MRGPRX	Mas related G protein coupled receptors X
PLCγ	Phospholipase γ
IP3	Inositol triphosphate
PIP3	Phosphatidylinositol(3,4,5)-bisphosphate
PDK1	Phosphoinositide-dependent kinase 1
ORAI-1	Ca^{2+} release-activated calcium channel protein 1

Author contributions

Yang Zhao and Zhongcheng Liu conceptualized, designed and wrote the manuscript. Yang Zhao performed experiments. Xiangsheng Li, Yuxin Shao, Yizhao Sun contributed to the animal test. Yang Zhao, Jianzhou Chu, Yanfen Zhang, Zhongcheng Liu revised the manuscript carefully for important intellectual content. All authors read and approved the final manuscript.

Conflicts of interest

The authors declare that there is no conflict of interest.

Acknowledgements

This work was supported by Key R & D projects in Hebei Province [grant number 20372702D]; Hebei Province Natural Science Foundation [grant number H2019201455, H2020201018]; and Post-graduate's Innovation Fund Project of Hebei University [grant number HBU2021ss073].

 This journal is © The Royal Society of Chemistry 2021

Published on 26 June 2021. Downloaded on 7/6/2021 4:12:49 AM.

References

1 R. Coombs and P. Gell, The classification of allergic reactions underlying disease, *Clin. Aspects Immunol.*, 1963, 317–317.
2 P. Lieberman, Mechanisms of anaphylaxis beyond classically mediated antigen and IgE induced events, *Ann. Allergy, Asthma, Immunol.*, 2017, **118**, 246–248.
3 D. Spoerl, P. Roux-Lombard, T. Harr, *et al.*, Non-IgE-dependent hypersensitivity to rocuronium reversed by sugammadex: report of three cases and hypothesis on the underlying mechanism, *Int. Arch. Allergy Immunol.*, 2016, **169**, 256–262.
4 J. Ye, H. Piao, J. Jiang, *et al.*, Polydatin inhibits mast cell-mediated allergic inflammation by targeting PI3K/Akt, MAPK, NF-κB and Nrf2/HO-1 pathways, *Sci. Rep.*, 2017, **7**, 11895.
5 S. Han, L. Sun, F. He, *et al.*, Anti-Allergic activity of glycyrrhizic acid on IgE-mediated allergic reaction by regulation of allergy-related immune cells, *Sci. Rep.*, 2017, **7**, 7222.
6 Y. Ding, D. Che, C. Li, *et al.*, Quercetin inhibits Mrgprx2-induced pseudo-allergic reaction via PLCγ-IP3R related Ca^{2+} fluctuations, *Int. Immunopharmacol.*, 2019, **66**, 185–197.
7 S. H. Wu, D. G. Wu and Y. W. Chen, Chemical constituents and bioactivities of plants from the genus Paeonia, *Chem. Biodiversity*, 2010, **7**, 90–104.
8 H. X. Wu, J. Y. Chen, Q. T. Wang, *et al.*, Expression and function of β-arrestin 2 stimulated by IL-1β in human broblast-like synoviocytes and the effect of paeoniflorin, *Int. Immunopharmacol.*, 2012, **12**, 701–706.
9 T. Chen, Z. P. Guo, X. Y. Jiao, *et al.*, Peoniflorin suppresses tumor necrosis factor-alpha induced chemokine production in human dermal microvascular endothelial cells by blocking nuclear factor-kappaB and ERK pathway, *Arch. Dermatol. Res.*, 2011, **303**, 351–360.
10 L. N. Ji, X. L. Hou, W. H. Liu, *et al.*, Paeoniflorin inhibits activation of the IRAK1-NF-κB signaling pathway in peritoneal macrophages from lupus-prone MRL/lpr mice, *Microb. Pathog.*, 2018, **9**, 223–229.
11 X. Kong, D. Leng, G. Liang, *et al.*, Paeoniflorin augments systemic Candida albicans infection through inhibiting Th1 and Th17 cell expression in a mice model, *Int. Immunopharmacol.*, 2018, **60**, 76–83.
12 Y. Zhang, S. Hu, S. Ge, *et al.*, Paeoniflorin inhibits IgE-mediated allergic reactions by suppressing the degranulation of mast cells though binding with FcεRI alpha subunits, *Eur. J. Pharmacol.*, 2020, **886**, 173415.
13 J. Wang, Y. Zhang, J. Wang, *et al.*, Paeoniflorin inhibits MRGPRX2-mediated pseudo-allergic reaction via calcium signaling pathway, *Phytother. Res.*, 2020, **34**, 401–408.
14 B. Lee, Y. W. Shin, E. A. Bae, *et al.*, Antiallergic effect of the root of Paeonia lactiflora and its constituents paeoniflorin and paeonol, *Arch. Pharm. Res.*, 2008, **31**, 445–450.
15 J. W. Tan, D. A. Israf, H. H. Harith, *et al.*, Anti-allergic activity of 2, 4, 6-trihydroxy-3-geranylacetophenone (tHGA) via attenuation of IgE-mediated mast cell activation and inhibition of passive systemic anaphylaxis, *Toxicol. Appl. Pharmacol.*, 2017, **319**, 47–58.
16 B. D. McNeil, P. Pundir, S. Meeker, *et al.*, Identification of a mast-cell-specific receptor crucial for pseudo-allergic drug reactions, *Nature*, 2015, **519**, 237–241.
17 J. Wang, Y. Zhang, S. Hu, *et al.*, Resveratrol inhibits MRGPRX2-mediated mast cell activation via Nrf2 pathway, *Int. Immunopharmacol.*, 2021, **93**, 107426.
18 M. Camps, C. Hou, D. Sidiropoulos, *et al.*, Stimulation of phospholipase C by guanine-nucleotide-binding protein beta gamma subunits, *FEBS J.*, 1992, **206**, 821–831.
19 P. Y. Zheng, X. R. Geng, J. Y. Hong, *et al.*, Regulating Bcl2L12 expression in mast cells inhibits food allergy, *Theranostics*, 2019, **9**, 4982–4992.
20 D. Chatterjea, A. Wetzel, M. Mack, *et al.*, Mast cell degranulation mediates compound 48/80-induced hyperalgesia in mice, *Biochem. Biophys. Res. Commun.*, 2012, **425**, 237–243.
21 Y. Xu, N. Guo, D. Dou, *et al.*, Proteomics study on nonallergic hypersensitivity induced by compound 4880 and ovalbumin, *PLoS One*, 2016, **11**, e0148262.
22 J. Yu, Y. Yang, L. Ying, *et al.*, Paeoniflorin inhibits mast cell activation and degranulation through PI3K/AKT/m-TOR signaling pathway, *Chin. J. Clin. Pharmacol. Ther.*, 2019, **24**, 961–968.
23 G. Wang and N. Cheng, Paeoniflorin inhibits mast cell-mediated allergic inflammation in allergic rhinitis, *J. Cell. Biochem.*, 2018, **119**, 8636–8642.
24 X. Zhenjiang, W. Lixin, D. Yuzhi, *et al.*, Effect of the Tibetan medicine Zuotai on Degranulation and Inflammatory Mediator Release in RBL-2H3 Cells, *Chem. Pharm. Bull.*, 2018, **66**, 818–821.
25 C. Walker, M. Kaegi, P. Braun, *et al.*, Activated T cells and eosinophilia in bronchoalveolar lavages from subjects with asthma correlated with disease severity, *J. Allergy Clin. Immunol.*, 1991, **88**, 935–942.
26 P. Rajagopalan, A. A. Dera, M. R. Abdalsamad, *et al.*, FPX-113 attenuates inflammatory responses by deteriorating cytokines, neutrophil activity and mast cell degranulation via Akt/ NF- κB pathway, *Biologia*, 2020, **75**, 447–456.
27 S. Hendrix, P. Kramer, D. Pehl, *et al.*, Mast cells protect from post-traumatic brain inflammation by the mast cell-specific chymase mice mast cell protease-4[J], *FASEB J.*, 2013, **27**(3), 920–929.
28 L. Niu, J. Wei, X. Li, *et al.*, Inhibitory activity of narirutin on RBL-2H3 cells degranulation, *Immunopharmacol. Immunotoxicol.*, 2020, **43**, 1–9.
29 Y. Desheva, A. Mamontov, N. Petkova, *et al.*, Mast cell degranulation and histamine release during A/H5N1 influenza infection in influenza-sensitized mice, *Life Sci.*, 2020, **258**, 118230.
30 H. Ohtsu, Pathophysiologic Role of Histamine: Evidence Clarified by Histidine Decarboxylase Gene Knockout Mice, *Int. Arch. Allergy Immunol.*, 2012, **158**, 2–6.
31 D. Che, Y. Hou, Y. Zeng, *et al.*, Dehydroandrographolide inhibits IgE-mediated anaphylactic reactions via calcium

Published on 26 June 2021. Downloaded on 7/6/2021 4:12:49 AM.

signaling pathway, *Toxicol. Appl. Pharmacol.*, 2019, **366**, 46–53.

32 R. Liu, T. Zhao, D. Che, *et al.*, The anti-anaphylactoid effects of hydroxysafflor yellow A on the suppression of mast cell Ca^{2+} influx and degranulation, *Phytomedicine*, 2018, **48**, 43–50.

33 X. Yu, X. Sun, M. Zhao, *et al.*, Propofol attenuates myocardial ischemia reperfusion injury partly through inhibition of resident cardiac mast cell activation, *Int. Immunopharmacol.*, 2018, **54**, 267–274.

34 F. Yang, Y. Li, X. Sheng, *et al.*, Paeoniflorin treatment regulates TLR4/NF-κB signaling, reduces cerebral oxidative stress and improves white matter integrity in neonatal hypoxic brain injury, *Korean J. Physiol. Pharmacol.*, 2021, **25**, 97–109.

35 Y. Zhou, X. Liu, Y. Gao, *et al.*, Paeoniflorin affects hepatocellular carcinoma progression by inhibiting Wnt/β-catenin pathway through downregulation of 5-HT1D, *Curr. Pharm. Biotechnol.*, 2020, **21**, 1–9.

36 S. Fang, W. Zhu, Y. Zhang, *et al.*, Paeoniflorin modulates multidrug resistance of a human gastric cancer cell line via the inhibition of NF-kappaB activation, *Mol. Med. Rep.*, 2012, **5**, 351–356.

37 S. J. Beavitt, K. W. Harder, J. M. Kemp, *et al.*, Lyn-deficient mice develop severe, persistent asthma: Lyn is a critical negative regulator of Th2 immunity, *J. Immunol.*, 2005, **175**, 1867–1875.

38 S. Y. Shim, Suppressive Effects of Vaccinium angustifolium Root Extract via Down-Regulation of Activation of Syk, Lyn, and NF-κB in FcεRI-Mediated Allergic Reactions, *Prev. Nutr. Food Sci.*, 2018, **23**, 30–34.

39 M. R. Woolhiser, Y. Okayama, A. M. Gilfillan, *et al.*, IgG-dependent activation of human mast cells following up-regulation of FcγRI by IFN-γ, *Eur. J. Immunol.*, 2015, **31**, 3298–3307.

40 G. Gomez, C. Gonzalez-Espinosa, S. Odom, *et al.*, Impaired FcεR I-Dependent Gene Expression and Defective Eicosanoid and Cytokine Production as a Consequence of Fyn Deficiency in Mast Cells, *J. Immunol.*, 2005, **175**, 7602–7610.

41 V. Parravicini, M. Gadina, M. Kovarowa, *et al.*, Fyn kinase initiates complementary signals required for IgE-dependent mast cell degranulation, *Nat. Immunol.*, 2002, **3**, 741–748.

42 A. M. Gilfillan, J. Rivera, *et al.*, The tyrosine kinase network regulating mast cell activation, *Immunol. Rev.*, 2009, **228**, 149–169.

43 X. Wang and Y. Liu, Regulation of innate immune response by MAP kinase phosphatase-1, *Cell. Signalling*, 2007, **19**, 1372–1382.

44 T. A. Trinh, Y. H. Seo, S. Choi, *et al.*, Protective Effect of Osmundacetone against Neurological Cell Death Caused by Oxidative Glutamate Toxicity, *Biomolecules*, 2021, **11**, 328.

45 V. P. Krymskaya, M. J. Orsini, A. J. Eszterhas, *et al.*, Mechanisms of Proliferation synergy by receptor tyrosine kinase and G protein-couple deceptor activation in human airway smooth muscle, *Am. J. Respir. Cell Mol. Biol.*, 2000, **23**, 546–554.

46 H. K. Faaaai, A. Naranjo, M. Smelkinson, *et al.*, Mechanical Activation of ADGRE2 Causes Calcium-dependent Activation of PI3K and MAPK Pathways Driving Mast Cell Degranulation and PGD2 Production, *J. Allergy Clin. Immunol.*, 2020, **145**, AB186.

47 P. D. Leitner, I. Vietor, L. A. Huber, *et al.*, Fluorescent thermal shift-based method for detection of NF-κB binding to double-stranded DNA, *Sci. Rep.*, 2021, **11**, 2331–2331.

48 J. Y. Kee, Y. D. Jeon, D. S. Kim, *et al.*, Korean Red Ginseng improves atopic dermatitis-like skin lesions by suppressing expression of proinflammatory cytokines and chemokines in vivo and in vitro, *J. Ginseng Res.*, 2017, **41**, 134–143.

49 J. Y. Kee and S. H. Hong, Ginsenoside Rg3 suppresses mast cell-mediated allergic inflammation via mitogen-activated protein kinase signaling pathway, *J. Ginseng Res.*, 2019, **43**, 282–290.

50 L. Li, G. Jin, J. Jiang, *et al.*, Cornuside inhibits mast cell-mediated allergic response by down-regulating MAPK and NF-κB signaling pathways, *Biochem. Biophys. Res. Commun.*, 2016, **473**, 408–414.

51 H. P. Zhang, Y. X. Sun, Z. Lin, G. Yang, J. Q. Liu, L. H. Mo, X. R. Geng, Y. N. Song, H. T. Zeng, M. Zhao, G. S. Li, Z. G. Liu and P. C. Yang, CARsomes inhibit airway allergic inflammation in mice by inducing antigen-specific Th2 cell apoptosis, *Allergy*, 2020, **75**, 1205–1216.

52 Z. Aryan, M. Tavakol, A. A. Amirzargar, *et al.*, Polymorphisms of genes encoding interleukin-4 and its receptor are associated with chronic idiopathic urticarial, *J. Allergy Clin. Immunol.*, 2014, **133**, 119.

53 D. G. Marsh, J. D. Neely and D. R. Breazeale, Linkage analysis of IL4 and other chromosome 5q31.1 markers and total serum immunoglobulin E concentrations, *Science*, 1994, **264**, 1152–1156.

54 E. J. Han, H. S. Kim, K. K. A. Sanjeewa, *et al.*, Sargassum horneri as a Functional Food Ameliorated IgE/BSA-Induced Mast Cell Activation and Passive Cutaneous Anaphylaxis in Mice, *Mar. Drugs*, 2020, **18**, 594.

55 A. Popov, I. Mirkov and M. Kataranovski, Inflammatory and immune mechanisms in contacthypersensitivity (CHS) in rats, *Immunol. Res.*, 2012, **52**, 127–132.

56 K. Matsui, X. Shi, S. Komori, *et al.*, Effects of anti-allergy drugs on Th1 cell and Th2 cell development mediated by Langerhans cells, *J. Pharm. Pharm. Sci.*, 2020, **23**, 412–421.

57 Y. H. Chuang, Y. H. Yang, S. J. Wu, *et al.*, Gene therapy for allergic diseases, *Curr. Gene Ther.*, 2009, **9**, 185–191.

58 M. Babina, S. Guhl, M. Artuc, *et al.*, Allergic FcεRI- and pseudo-allergic MRGPRX2-triggered mast cell activation routes are independent and inversely regulated by SCF, *Allergy*, 2018, **73**, 256–260.

59 B. D. Mcneil, P. Pundir, S. Meeker, *et al.*, Identification of a mast-cell-specific receptor crucial for pseudo-allergic drug reactions, *Nature*, 2014, **519**, 237–241.

60 H. Subramanian, K. Gupta and H. Ali, Roles of MAS-related G protein coupled receptor-X2 (MRGPRX2) on mast cell-

 This journal is © The Royal Society of Chemistry 2021

mediated host defense, pseudoallergic drug reactions and chronic inflammatory diseases, *J. Allergy Clin. Immunol.*, 2016, **138**, 700–710.

61 C. J. Occhiuto, A. K. Kammala, C. Yang, *et al.*, Store-Operated Calcium Entry via STIM1 Contributes to MRGPRX2 Induced Mast Cell Functions, *Front. Immunol.*, 2020, **10**, 3143.

62 D. E. Kim, K. J. Min, M. J. Kim, *et al.*, Hispidulin Inhibits Mast Cell-Mediated Allergic Inflammation through Down-Regulation of Histamine Release and Inflammatory Cytokines, *Molecules*, 2019, **24**, 2131.

63 Z. Ovary, Passive cutaneous anaphylaxis in the mice, *J. Immunol.*, 1958, **81**, 355–357.

64 E. J. Han, H. S. Kim, K. K. A. Sanjeewa, *et al.*, Eckol from Ecklonia cava Suppresses Immunoglobulin E-mediated Mast Cell Activation and Passive Cutaneous Anaphylaxis in Mice (Running Title: Anti-Allergic Activity of Ecklonia cava), *Nutrients*, 2020, **12**, 1361.

65 S. W. Hwang, X. Sun, J. H. Han, *et al.*, Fermentation-mediated enhancement of ginseng's anti-allergic activity against IgE-mediated passive cutaneous anaphylaxis in vivo and in vitro, *J. Microbiol. Biotechnol.*, 2018, **28**, 1626–1634.

Published on 26 June 2021. Downloaded on 7/6/2021 4:12:49 AM.